Geochemistry of vent fluids from the Daxi Vent Field, Carlsberg Ridge, Indian Ocean: Constraints on subseafloor processes beneath a non-transform offset

Xueting Wu [a, b]†, Xiqiu Han [a, b, c *]†, Yejian Wang [b*], Dieter Garbe-Schönberg [d], Mark Schmidt [e], Zhaohui Zhang [a], Zhongyan Qiu [b], Tong Zong [f], Peng Zhou [b], Xing Yu [b], Jiqiang Liu [b], Hongming Luo [b], DY33 and DY38 Leg 1 Shipboard Scientific Party

Affiliations

[a] *Ocean College, Zhejiang University, Zhoushan 316021, China*

[b] *Key Laboratory of Submarine Geosciences & Second Institute of Oceanography, Ministry of Natural Resources, Hangzhou 310012, China*

[c] *School of Oceanography, Shanghai Jiao Tong University, Shanghai 200240, China*

[d] *Institute of Geosciences, Kiel University, Kiel 24118, Germany*

[e] *GEOMAR, Helmholtz Centre for Ocean Research Kiel, Kiel 24148, Germany*

[f] *College of Architectural Engineering, Weifang University, Weifang 261061, China*

†These authors contributed equally to this work

[*]Corresponding author:

Xiqiu Han, e-mail address: xqhan@sio.org.cn, tel: +86-571-81963004

Yejian Wang, e-mail address: yjwang@sio.org.cn, tel: +86-571-81061785

Abstract

The Daxi Vent Field (DVF) is located on a neo-volcanic ridge within a non-transform offset at water depths of ~3500m, on the Carlsberg Ridge, northwest Indian Ocean. In 2017, we investigated this site using the submersible *Jiaolong* and collected two fluid samples from orifices of chimneys named "Buddha's Hands" and "A1", about 37 m apart. Their *in-situ* measured temperatures are 273 °C and 272 °C, respectively. The Buddha's Hands fluid is highly Cl-enriched (928 mM), while the A1 fluid is Cl-depleted (303 mM) indicateing that they have undergone phase separation. The segregated phases must have remixed during the ascent because the vapor and brine phases sampled cannot be produced by the same phase separation history without other processes. Olivine-rich and/or ultramafic mantle rocks must have been involved during the hydrothermal circulation as evidenced by high dissolved H_2 (7.07 mM) and methane (0.884 mM) concentrations, a depletion in B relative to seawater, high Ca and low K, and large positive Eu anomalies. The Fe content in Buddha's Hands fluid is extremely high (11,900 μM) as a result of phase separation, while the Cu concentrations in both fluids are relatively low due to entrainment of seawater which results in precipitation of Cu-rich sulfides in the subseafloor. The concentrations of Zn, Ag, Ga, Sn, Sb, and Cd in A1 vent fluid are significantly elevated due to generation of acidity and remobilization of these elements as Cu-rich sulfides are deposited. The subseafloor processes and associated geochemistry of hydrothermal fluids at the DVF are distinct from other mid-ocean ridge hydrothermal systems due to the specific geologic setting. Hence a hybrid model of hydrothermal circulation is proposed. This study broadens our understanding of the hydrothermal processes occurring in areas of NTO setting and provides more information on mass fluxes discharging from hydrothermal systems and the formation of sulfide deposits.

Keywords: Daxi Vent Field; Carlsberg Ridge; Non-Transform Offset; vent fluid geochemistry; serpentinization

1. Introduction

Since the first discovery of seafloor hydrothermal vents in the late 1970s, more than 700 submarine hydrothermal fields have been identified in a great variety of tectonic setting ranging from mid-ocean ridges (MOR) to back-arc basins, submerged volcanic arcs, and hot-spot-related intraplate volcanoes (Beaulieu and Szafrański, 2020; Edmond et al., 1979; Baker and German, 2004; de Ronde and Stucker, 2015; Hannington et al., 2005). During hydrothermal circulation, seawater penetrates into the fractured oceanic crust, is heated and reacts with the host rock. Thereby it is transformed into a hot, reducing, metal-rich, Mg- and sulfate- poor hydrothermal fluid that ultimately is expelled into ocean (Tivey, 2007). Hydrothermal convection plays a crucial role in exchange of material and heat between the oceans and the oceanic crust.

Fluid-rock interactions and phase separation have a first order effect on the geochemical composition of hydrothermal fluids (German and Seyfried, 2014). In general, arcs and back-arc systems are characterized by high diversity of host rocks ranging from basaltic andesite, andesite, dacite, and even rhyolite make-up (de Ronde and Stucker, 2015). This results in increased variability of fluid compositions compared to those at the mid-ocean ridge systems. Ultramafic-hosted systems are common along slow- and ultra-slow spreading ridges with increasing number of sites being discovered (Fouquet et al., 2010). Serpentinization, a specific water-rock interaction in the ultramafic rock settings leads to the characteristic geochemistry of fluids compared to those at mafic-hosted rock settings, e.g. high CH_4 and H_2 contents (Fouquet et al., 2010). The water-rock interactions occur over a wide range of pressure and temperature from the seafloor to the deep reaction zone. Phase separation commences as the solution reaches the two-phase boundary, with generation of a vapor phase and a brine phase (Bischoff and Pitzer 1989; Driesner and Heinrich 2007). The compositions of high-temperature fluids is further modified by partitioning of elements between the vapor and brine phases by formation of chloride complexes (Driesner and Heinrich 2007). Moreover, magmatic inputs and entrainment of seawater during subsurface passage further complicates the vent fluid chemistry (Bach et al. 2003; Paulick and Bach 2006). The complexity of hydrothermal systems has made the nature and relative influence of these variables the focus of much debate and details are still unclear how much hydrothermal fluxes contribute to the elemental budget of the oceans.

The Daxi vent field was discovered on the saddle of a neo-volcanic ridge in a non-transform offset (NTO) area. NTOs located at the end of ridge segments usually have a thin and cold oceanic crust underlying because of relatively low magma supply. This results in pervasive faulting and an open hydrologic setting (Gràcia et al, 1997, 2000). Moreover, large-displacement and low-angle detachment faults can develop in NTOs and excavate lower crust and mantle rocks charaterized by gabbro and peridotite (McCaig et al., 2010). To our knowledge, only nine vent fields associated with NTOs have been reported in the world's ocean, seven of which are situated within ultramafic rock settings (i.e. Rainbow, Nibelungen, Menez Hom, Saldanha, Yokoniwa, Ghost City and Clamstone; Beaulieu and Szafrański, 2020; Charlou et al., 2002; Schimidt et al., 2011; Fouquet et al., 2010; Dias and Barriga, 2006; Li et al., 2018; Cherkashov et al., 2010; Lartaud et al., 2010; Lartaud et al., 2011; Fujii et al., 2016). These setting provide the scant information available hydrothermal circulation in ultramafic-hosted systems. We speculate that hydrothermal fluids at NTOs should have undergone a complex evolution involving multiple consecutive or concurrent processes, but only at two sites high temperature fluids have been sampled and analyzed (i.e. Rainbow and Nibelungen; Charlou et al.,2002; Schmidt et al., 2011). They differ in composition due to their different tectonic setting and assumed subseafloor processes.

The DVF samples add to our understanding of hydrothermal activity at NTOs, as well as their role in material fluxes and energy flow in the oceans. The vent fluids from the DVF were sampled in 2017 by the Human Operated Vehicle-HOV '*Jiaolong*' during the DY38-I Expedition. Here, we present results on the geochemistry of hydrothermal fluids, which allow a more straightforward interpretation of water-rock interactions, and discuss the constraints on the geochemical processes during fluid circulation beneath the NTO. This study expands the global dataset for hydrothermal vent fluid compositions and may also provide a clue for the seafloor massive sulfide exploration of NTOs in the world ocean.

2. Background

Geochemical investigations of sulfides, of water column plumes, of associated vent fauna as well as the bathymetric, visual and geophysical data obtained during previous cruises to the Daxi Vent Field provide vast background on the structural setting from which the fluid samples originate (Wang et al., 2021). Compared to the other hydrothermal fields reported in the Indian Ocean, the DVF is located on a saddle of a neo-volcanic ridge Daxi Ridge between two second-order ridge segments at 6°48′N and 60°10′E, at water depths ~3500 m (Fig. 1A; Wang et al., 2021). At the DVF, actively venting chimneys are clustered inside the Central Mound, which is ~180 m wide and ~50 m high (Fig. 1B). Eight active chimney clusters higher than 10 m were found within an area ~80 m wide. The large chimney cluster, named Buddha's Hands, is about 20 m high and located in the east of Central Mound. Five slender and finger-like pipes about ~1 m high developed at the top, vigorously emanating clear fluids. Beehive structures venting grayish-white diffuse fluid developed at the base of chimney clusters (Fig. 2A). Minerals in the chimneys are dominated by Fe-rich and Zn-rich sulfides (Wang et al., 2021). The A1 chimneys occur to the southwest of the Buddha's Hands. It consists of dozens of small chimneys and several large chimneys up to ~5 m tall (Fig. 2B). The small chimneys range from a few to tens of centimeters in width, and less than one meter to several meters in height. The less vigorous diffuse fluids are widespread distributed among the chimneys and support patches of *Alvinocaridid* shrimps and *Bythograeid* crabs. The NE Mound is located ~30 m northeast of Central Mound and an extinct siliceous chimney ~2 m high has developed at this site.

Two high-angle NNW-SSE trending normal faults with opposite dip angles delimit each flank of the neo-volcanic ridge. The presence of pervasive fractures and faults enhance crustal permeability. Altered brownish basalt fragments are present in the vicinity. Basalt lavas, brecciated pillows, and sediment pockets which are slightly altered were found towards the southeast about 100 m away from the venting sites. No ultramafic rocks have been observed during the cruise. However, the nature of topographic highs adjacent to the NTO needs further exploration (Fig. 1A)

3. Samples and Methods

3.1 Sample collections

Two vent fluids samples were collected from the orifices of a slender chimney at the Buddha's Hands and a beehive chimney at A1 using a 160-ml titanium alloy gas-tight isobaric (IGT) sampler via a titanium snorkel (designed by State Key Laboratory of Fluid Power Transmission and Control, Zhejiang University, Wu et al., 2014; Table 1; Figs. 2C, D). A thermocouple was tied to the snorkel for real-time measurement of *in-situ* temperature. The maximum temperatures recorded were 273 °C at Buddha's-Hands and 272 °C at A1. Detailed description of sampling method can be found in Wu et al., (2014).

The samples were processed immediately upon recovery on deck. About 1 ml of fluid was taken for pH determination on board at room temperature (25 °C) using a Meinsberg TM39 SM pH Meter. Fluid aliquots for measurement of non-volatile dissolved species were stored in acid-washed, high-density polyethylene (HDPE) Nalgene bottles and frozen at -80 °C. Aliquots for volatile species analysis were transferred isobarically into 40ml titanium alloy gas-tight sample tubes and stored at 4 °C. Precipitates that formed in the samplers due to the cooling or mixing with entrained seawater were washed into an acid-cleaned 100 ml HDPE bottle with ultrapure Milli-Q water.

A background seawater sample collected at 5°5′57″N and 62°3′14″E using a Niskin bottle at 2756 m (Station 43V-CR-S016-CTD05) during a later cruise was used for comparation. The sample was acidified with thermally distilled HNO_3, and stored in an acid-cleaned 500 ml HDPE bottle at 4 °C for analysis of major and trace elements.

3.2 Analytical methods

Particles from black smoker fluids collected on membrane filters were leached with 5 ml freshly prepared aqua regia and 1 ml concentrated HF into 15 ml perfluoralkoxy (PFA) vials. Concentrations of major and minor elements (Cl, Br, B, Si, Na, K, Ca, Mg, Sr) of particle and fluid samples collected in HDPE bottles were determined on an inductively coupled plasma optical emission spectrometry (ICP-OES, Spectro Ciros SOP) at Kiel University. Samples were 10-fold diluted with 5% (v/v) HNO_3 and spiked with 5 mg/l Y for internal standardization. International seawater reference materials IAPSO (Atlantic Seawater Salinity Standard), NASS-5 (trace elements in seawater, NRC-CNRC), LGC6019 (Thames river water, LGC) and an in-house standard of Logatchev hydrothermal fluid were used for checking accuracy of the results. Analytical precision was monitored by repeat analyses of samples and found to be better than 2 %RSD.

Trace elements (Ge, Al, Rb, Cs, Ba, Fe, Mn, Co, Ni, Cu, Zn, Cd, Ag, Ga, In, Sn, Pb, Tl, As, Se, Sb, Mo, W, U) were determined on a high resolution sector-field ICP-MS (Thermo Element XR) at Kiel University, after 50-fold dilution with 5% (v/v) HNO_3 and spiking with 2.5 ng/ml Be, Y, Re. Elements Ga, Ge, As, Se, and Te were measured in high resolution mode (RP 10,000), all first row transition metals in medium resolution (RP 4,000), and the remaining elements in low resolution mode. International seawater reference materials IAPSO, NASS-5 (trace elements in seawater, NRC-CNRC), LGC6019 (Thames river water, LGC) and an in-house standard of Logatchev hydrothermal fluid were used for checking accuracy of the results. Analytical precision was monitored by repeat analyses of samples and found to be better than 5-10 % RSD for elements Li, V, Cr, Cu, Zn, As, Rb, Sr, Mo, Ag, Cs, Ba, Hg, U, except elements with very low concentrations near their limit of detection (Cd, Sn, Sb, Te, Tl, Co, Ni). All acids were of sub-boiled quality and all PFA labware had been pre-conditioned following a multi-step cleaning protocol.

Sulphate concentrations of the fluid samples were measured on a ion chromatography (Metrohm 761 IC). The chromatograph was equipped with a conductivity and an UV-detector. Filtrated fluid samples were injected on a Metrosep A Supp5 column and separated by $NaCO_3$/$NaHCO_3$ solution. The analytical precision was ±2 % based on repeated analysis of IAPSO seawater standard. Dissolved gases were extracted from 40 ml of hydrothermal fluid by connecting the pressure containers to a high-vacuum apparatus, where the liquid phase was acidified to pH<2 under vacuum. Total released gas volume was calculated by using the known inner volume of the vacuum device at measured pressure and temperature. The gas composition was determined on a Shimadzu gas chromatograph (GC2014) equipped with a flame ionization detector and a thermal conductivity detector, a HayeSep Q 80/100 column, and using helium as carrier gas at 5 ml/min. The analytical precision of ±2-10 % was achieved when measuring standard single gas mixtures in helium and synthetic air.

4. Results

4.1 Non-volatile dissolved species

4.1.1 Magnesium and sulfate

Measured data and the calculated end-member compositions of vent fluids are presented in Tables 2-4. Magnesium and SO_4^{2-} are known to be quantitatively removed during water/rock interaction in most hydrothermal systems as also experimentally shown, and hence there should be no Mg in endmember hydrothermal fluids (Mottl and Holland, 1978; Zhang , 2020). The Mg concentrations of both fluid samples at the DVF are 27.5 and 44.3 mM, suggesting that they have been mixed with 53% and 84% of seawater, given seawater Mg= 52.6 mM. The composition of hydrothermal end-member SO_4^{2-} and the other non-volatile dissolved species and volatile aqueous species discussed below were calculated using a least squares regression of their measured concentrations and Mg and then extrapolating measured values to zero Mg. The calculated endmember SO_4^{2-} of the Buddha's-Hands and the A1 fluid are -5.88 mM and

8.22 mM, respectively, indicating that SO_4^{2-}-removal during the mixing of hydrothermal fluid with SO_4^{2-}-rich seawater in the upflow zone. Formation of barite and/or anhydrite is likely, and the SO_4^{2-} content could also have been slightly affected by oxidation of H_2S during storage.

4.1.2 Chloride and bromine

The calculated endmember Cl-concentration in the Buddha's Hands fluid is 928 mM, significantly higher than that in normal seawater, whereas it is 303 mM in the A1 fluid, significantly lower than that in seawater (Table 2). The same trend is also found in Br, with 1466 μM in the Buddha's-Hands fluid and 354 μM in the A1 fluid. When normalized to Cl, the Br/Cl ratio is close to that of seawater (1.54×10^{-3}) in the Buddha's Hands fluid (1.58×10^{-3}), but lower than seawater in the A1 fluid (1.17×10^{-3}).

4.1.3 Alkali, alkaline earth elements, boron and silicon

The calculated endmember concentrations of alkali elements and alkaline earth elements in the sampled fluids are highly elevated compared to seawater (Table 2). When normalized to Cl, the endmember Na/Cl ratios obtained from Buddha's Hands and A1 are similar, with their values of 0.802 and 0.809, lower than that of seawater (0.861). Endmember K/Cl, Li/Cl and Rb/Cl ratios are about 2-, 20-, and 10- times higher than those in seawater, respectively, with the Buddha's-Hands fluid slightly higher than those in the A1 fluid. Endmember Cs/Cl and Ca/Cl ratios are about 30-, and 4-times higher than seawater, respectively, with the Buddha's-Hands fluid slightly lower than those in the A1 fluid. Endmember Sr/Cl ratios are 0.219×10^{-3} in the Buddha's Hands fluid and 0.111×10^{-3} in the A1 fluid. The former is slightly higher than in seawater (0.159×10^{-3}), the latter is slightly lower. Endmember Ba concentrations are 5.53 μM and 7.79 μM in the Buddha's Hands and A1 fluids, respectively.

B behaves differently. Endmember B/Cl ratios of both samples are about 2 times lower than that of seawater. Endmember SiO_2 concentrations in the Buddha's Hands (1.17 mM) and A1 fluid (1.39 mM) are slightly higher than that of seawater (0.0850 mM), but at the lower end of reported SiO_2 concentrations in high-temperature hydrothermal fluids (James et al. 2014; Seyfried et al. 2011)

4.1.4 Transition metals

Transition metals tend to precipitate as sulfide minerals during the sampling process when seawater is entrained and cools. To correct for the effects of sulfide precipitate formation within the fluid samplers, reported metal contents were generally obtained by summation of the dissolved and precipitated metal fractions inside a given sampler. However, we found that the reconstructed transitional metal concentrations (e.g. Fe, Cu, Zn, Co, etc) were unreasonably high in the DVF fluids, most likely due to entrained chimney particles. Apparently, such reconstruction was problematic. If the mixing occurred during sampling, then substantial sulfide precipitation may have occurred in the samplers, but would have been overshadowed by the chimney particles that were also collected. Therefore, we used the metal contents in the filtrate to calculate the endmember concentrations of transition metals. As some of the metals load may have been lost by sulfide precipitation, the calculated endmember values are taken as the lower limit.

All transition metals in both samples are strongly elevated compared to those in seawater. Concentrations of Fe, Mn, Cu, and Co are much higher in the Buddha's-Hands fluid than those in the A1 fluid. Other metals like Zn, Ga, Cd, Ag and Sn co-vary with each other and are strongly enriched in the A1 fluid.

4.1.5 Rare earth elements

Concentrations of rare earth elements (REE) are strongly enriched in the DVF samples compared to those in seawater (Table 4). The chondrite-normalized distribution pattern is characterized by an enrichment of LREE over HREE and pronounced positive Eu anomalies (Buddha's Hands: Eu/Eu* = 133, A1: Eu/Eu* = 88). Their magnitude in the DVF fluids are among the highest ever reported for hydrothermal systems (Charlou et al., 2000; Von Damm et al., 1998, Schmidt et al., 2017).

4.2 Volatile aqueous species

Only the Buddha's Hands fluid was analyzed for its volatile aqueous species. Endmember H_2 abundance of 7.07 mM is significantly higher than observed in other mafic-hosted hydrothermal systems with normally less than 1 mM. Endmember CH_4 content (0.884 mM) is also typically higher than in the most MOR systems (Edmonds, 2010). The H_2S content is below detection limits indicating it is lower than that in other mafic-hosted systems, which usually ranges from 4 to 6 mM (Douville et al., 2002). The possibility of loss of sulfide during sample recovery and/or oxidation during storage cannot be ruled out.

4.3 Particles

The particles collected in the HDPE bottles from the Buddha's Hands and A1 sites are quite different in their chemical composition (Table 5). The former is dominated by Fe and Cu, while particles from A1 are dominated by Zn and Fe, with minor Cu. The trace metals Co, Ni, As, Se, Al and V are more enriched in the Buddha's-Hands fluid, while Pb, Cd, Ga and Sn are more enriched in the A1 fluid. The particulate Ba contents in both samples are extremely low.

5. Discussion

5.1 Phase separation and the inferred p-T conditions

One of the striking features of the two hydrothermal fluids from the Daxi Vent Field (DVF) is their very different Cl concentration; e.g. 928 mM versus 303 mM, with seawater at 542 mM. This significant difference is also apparent in the raw data prior to calculating endmember concentrations. Enrichments or depletions of Cl relative to seawater in vent fluids within mafic and ultramafic-hosted hydrothermal system are typically attributed to phase separation (Von Damm, 1990, 1995). The Buddha's Hands fluid could represent a brine phase, while the A1 fluid cannot be the conjugate vapor phase as explained below.

According to the phase diagram of seawater (Fig. 3) and the water depth at the Daxi Vent Field (3450 m, 345 bars), the corresponding temperature for phase separation at this depth would be at least 425 °C, which is hotter and deeper than the critical point for seawater at 407 °C and 298 bars represented by the NaCl-H_2O system. It suggests that the hydrothermal fluid phase separation occurred under supercritical conditions (German et al., 2014). Based on the isotherms of the vapor-liquid region in the NaCl-H_2O system (Fig. 4), the Cl content in co-existing vapor and brine phases at given p-T conditions can be calculated. Obviously, the salinities of the two fluid samples cannot be produced within the same phase separation history. Moreover, when projecting the salinity of both fluid samples to higher temperature isotherms, both of them even lie at the vapor side of solvus. Therefore, the two compositions of the DVF fluids cannot be produced by phase separation at any conditions below the seafloor. However, the similar alkalis/Cl and alkali earth/Cl ratios between the Buddha's Hands and A1 fluids suggest that they have a common source (Table 3). Thus, we deduce that the salinities of venting fluids at the DVF might have been modified by re-mixing of variable proportions of segregated vapor and brine in the subseafloor such that the Cl content was elevated in the vapor phase, and reduced in the brine phase. In addition, we can also find that the Br/Cl ratio of A1 fluid is lower than the seawater value. A lower Br/Cl relative to seawater indicates the presence of halite dissolution because Br is preferentially excluded from the halite structure (Berndt and Seyfried, 1990; Oosting and Von Damm, 1996). That is probably why A1 fluid has the lower ratios of K/Cl, Li/Cl, Rb/Cl, B/Cl, but higher Na/Cl ratio relative to the Buddha's Hands fluid. Therefore, the A1 fluid chemistry was affected by halite dissolution during its ascent after phase separation.

To determine the p-T conditions for hydrothermal circulation, a Si-Cl geothermometer is commonly used, based on the assumption that quartz and fluid reached equilibrium at depth and the Si and Cl concentrations do not change during the following ascent (Foustoukos and Seyfried, 2007). However, this scenario is not applicable for the DVF fluids because the anomalously low concentrations of silica (1.17 to 1.39 mM) is outside the range of experimental data. Alternatively, a Fe/Mn geothermometer may be applied to reconstruct p-T conditions of the fluid's last equilibrium with greenschist facies rocks (Pester et al., 2011; Mottl et al., 1979; Rosenbauer and Bischoff, 1983). For the Buddha's Hands fluid, which has the highest endmember concentration of Mn with a Fe/Mn ratio of about 7.7, the calculated equilibrium temperature is 431 °C. However, as discussed in the following section 5.2, the Buddha's Hands fluids have been cooled by entrained seawater during its transport from the reaction zone to the seafloor and part of the Fe may have been precipitated as sulfides, causing a decrease of Fe/Mn ratio. Therefore, the calculated temperature of 431 ℃ for the reaction zone using the Fe/Mn geothermometer should be taken as the lower end. Assuming that phase separation happened at 431 ℃ and that the fluids interacted only minimally with the surrounding rocks during ascent from the phase separation zone, the predicted corresponding pressure should be 353 bars (Fig. 4). This implies that phase separation occurred in the depth of ~80 m below the seafloor. However, considering that the temperature in the reaction zone should be higher than 431 ℃, the possibility fluids phase separated deeper in this system cannot be precluded.

5.2 Mixing and cooling by entrained seawater and the deposition of sulfides

A minimum temperature of ~431 ℃ is predicted for the reaction zone, however, the *in-situ* measurement of venting fluids is only ~270 ℃. The significantly lowered temperature of hydrothermal fluids from the reaction zone to the seafloor at the DVF is attributed to the mixing with seawater during ascent, as conductive cooling is not an efficient mechamism for significant cooling due to rapid ascent of the fluid and the low thermal conductivity of the oceanic crust (Sleep and Morton, 1983). This may be related to the specific geologic setting of the DVF. NTOs are commonly characterized by low magma supply and pervasive faulting within a relatively thin oceanic crust (Gràcia et al., 1997, 2000), resulting in an open hydrologic regime beneath the DVF. This is supported by abundant fissures and fractures observed during submersible investigation (Wang et al., 2021). An important consequence of mixing of endmember fluids with seawater is the deposition of anhydrite and sulfide minerals. The calculated negative SO_4^{2-} endmember in the DVF fluids is a good indication that this process might have occured. However, the Ca/Cl ratios are still much higher than that in seawater and among the highest values ever reported in high-temperature submarine hydrothermal fluids (Fig. 5). The accompanied depletion in Na relative to seawater in both fluid samples suggest that albitization also occurred during water-rock interaction and contributed to the Ca addition from the destruction of anorthite (Berndt and Seyfried, 1993). However, this interpretation does not rule out differences in host rock lithologies, e.g. high Ca as signature of clinopyroxene alteration with Mg-Ca exchange (Boschi et al., 2008; Schmidt et al., 2007). In addition, the Ba concentrations in the Buddha's Hands and A1 fluid are extremely low compared to other hydrothermal systems. Most of Ba is still dissolved and the Ba content in solid material (particles) is extremely low. Thus, precipitation of barite might also have occurred in the subseafloor.

The endmember concentrations of Fe, Cu, Co, and Mn are higher in the Buddha's Hands fluid than those in the A1 fluid, while those of Zn, Ag, Ga, Sn, Sb, and Cd are lower. The higher concentrations of Fe, Cu, Co, and Mn in the high-Cl fluid underscore the importance of phase separation on metal contents. Strong enrichment in most of the transition and heavy metals related to phase separation has been observed in both mafic and ultramafic hydrothermal systems (Douville et al., 2002; Schmidt et al., 2017; Chavagnac et al., 2018; Webber et al., 2015). The metals preferentially partition into the brine during phase separation due to the formation of metal-chloro-complexes; this holds true especially for Fe whose divalent nature favors strong chloro-complexes (Douville et al., 2002; Pester et al., 2014; Seyfried et al., 2003).

The stability of metal-chloro-complexes depends strongly on pressure and temperature. The temperature-dependent rates of equilibration with sulfide minerals are the fastest for Cu, followed by Fe, Zn, and Mn (Seewald and Seyfried, 1990). As shown in Fig. 6, the endmember concentrations of Cu and Fe in the A1 fluid are strongly depleted relative to other hydrothermal systems with similar chlorinities. The Cu content is also extremely low in the Buddha's Hands fluid, whereas the Fe concentration is still extremely high (11,900 μM). Concentrations of Zn, Ag, Ga, Sn, Sb, and Cd are much higher in the A1 fluid than in the Buddha's Hands fluid and other known hydrothermal systems. Since the venting fluids at the DVF must have cooled from about 431 °C to 272 °C, the low Fe and Cu contents in the A1 fluid are likely resulted from the precipitation of Fe and Cu sulfides as the temperature decreased before venting. Large portions of ore-forming elements, especially Cu, Co, Fe, Ni, As, Se, Al and V were fixed in such sulfides, favoring the formation of large-size sulfide mineral deposits. An important consequence of the formation of Fe and Fe-Cu sulfide minerals beneath the seafloor is an increase of acidity, promoting the remobilization of Zn, Ag, Ga, Sn, Sb, and Cd from sphalerite that had previously precipitated (Tivey et al., 1995). Thus, the concentrations of Zn, Ag, Ga, Sn, Sb, and Cd became significantly elevated in the A1 fluid. The extremely low Cu in the Buddha's Hands fluid indicate that a large portion of Cu must have been fixed in Cu-sulfide minerals in the subseafloor. However, the extremely high Fe concentration (11916 μM) and the lower concentrations of Zn, Ag, Ga, Sn, Sb, and Cd relative to that in A1 fluid indicate that the metal remobilization has not significantly occurred to modify the fluid compositions.

The characteristics of the metal contents in the particles collected from the fluid sampler show a similar trend as the hydrothermal fluids. Particles obtained from Buddha's Hands fluid are dominated by Fe and Cu, whereas those from the A1 fluid are dominated by Zn with minor Fe and Cu. Trace metals Co, Ni, As, Se, Al and V are more enriched in particles from the Buddha's Hands fluid, while Pb, Cd, Ga, and Sn are more enriched in particles from the A1 fluid. Strong affinities of Co, Ni, As, Se, Al and V to Cu-Fe sulfides, and Pb, Cd, Ga, and Sn to Zn-rich sulfides are thereby confirmed. As the components of the chimney build-up, these sulfides may well inherit the fluid characteristics. Considering the difficulty in hydrothermal fluid collection, the circulation in a new hydrothermal field may be preliminarily inferred from the chemical composition of the sulfide chimneys.

5.3 Possible involvement of serpentinization on the pathway of hydrothermal circulation

The DVF fluids are characterized by a depletion of B (Fig. 5). Boron is commonly enriched in mafic-hosted hydrothermal systems (Seyfried et al., 1984), but a depletion taken as a fingerprint of ultramafic-hosted hydrothermal systems, because B is lost from seawater to serpentine minerals (substituting for Si) and brucite (adsorption) during serpentinization (Boschi et al., 2008; Schmidt et al. 2011). Therefore, the depletion in B in the DVF fluids may indicate that the existence of serpentinization somewhere along the path of subseafloor circulation. Pb and Cd in Buddha's Hands fluid are significantly lower than those in other basaltic-hosted hydrothermal systems, while Sn in the A1 fluid is high and comparable to that of the Rainbow field (Table 6; Schmidt et al., 2011). This phenomenon may also point to the involvement of ultramafic-rock interaction. During serpentinization of abyssal peridotite and/or olivine-rich gabbro, Pb and Cd in the fluid could be incorporated into serpentine minerals resulting in low Pb and Cd in the final fluid composition (Agranier et al., 2007). In contrast, strongly elevated Sn concentration in fluids of the DVF and other ultramafic-hosted systems may be due to its high incompatibility during igneous processes (Badullovich et al., 2017; Jochum et al., 1993). Ultramafic-hosted hydrothermal systems are commonly enriched in Au in their vent fluids as well (Keith et al., 2014). However, Au is below detection limit in the DVF fluids, suggesting that it may have co-precipitated with Cu and Co in the subseafloor induced by cooling during mixing with entrained seawater.

In addition to the chemical clues from trace elements, as discussed above, serpentinization might have been involved during hydrothermal circulation, and volatile dissolved species such as H_2, and CH_4, can provide further evidence. As shown in Fig. 7, the endmember H_2 abundance of the Buddha's-Hands fluid is as high as 7.07 mM, while it is usually lower than 1 mM in mafic-hosted hydrothermal systems. In contrast, the endmember abundance of H_2 in ultramafic-hosted hydrothermal systems is usually higher than 10 mM. The Kairei hydrothermal field (KHF) is an exception, which is supposed to be mafic-hosted but with the influence of serpentinization of olivine-rich gabbro resulting in a high endmember H_2 content from 2.5-8.2 mM (Gallant and Von Damm, 2006; Kumagai et al., 2008; Nakamura et al., 2008). The endmember CH_4 abundance in the Buddha's Hands fluid is 0.884 mM. For comparison, the endmember CH_4 abundance of mafic-hosted hydrothermal systems usually ranges from 0.3 mM to 1 mM, except those samples from the Main Endeavour field at Juan de Fuca Ridge which contain high CH_4 derived from its thickly sediment covered (Lilley et al., 2003). The endmember CH_4 abundance in typical ultramafic hydrothermal systems is usually around 2-3 mM, while the KHF fluid has an unusually low CH_4/H_2 ratio due to the relatively high fO_2 condition compared to serpentinization of typical abyssal peridotite (Nakamura et al., 2008). Therefore, the endmember CH_4 abundance of 0.884 mM in the Buddha's Hands sample is at the high end compared to those sediment-free mafic-hosted hydrothermal systems and close to the low end of ultramafic hydrothermal systems. The coupled enrichment in both H_2 and CH_4 in the DVF fluid is consistent with other ultramafic- hosted hydrothermal sites. In these hydrothermal systems, large amount of H_2 are generated during aqueous oxidation of ferrous ironbearing minerals. Accumulation of H_2 during serpentinization results in the generation of sufficiently strong reducing conditions that CO_2 can be reduced to CH_4 (Horita and Berndt, 1999; McCollom and Seewald, 2001; Klein et al., 2015). However, the physical conditions and reaction pathways of CH_4 formation remain incompletely understood. It has been predicted that the abiotic CH_4 was formed during active fluid circulation through a series of Fischer-Tropsch-type reactions (Berndt et al., 1996). With the further in-depth research, more works have shown that CH_4 in circulating fluid is more likely leached from fluid inclusions hosted in olivine-rich rocks where serpentinization occurs. This is confirmed to be a widespread process in upper mantle or lower oceanic crust (McDermott, 2015; Klein et al., 2019; Grozeva et al., 2020). The high H_2 and CH_4 contents in the Daxi fluid may be also controlled by this process. Therefore, it is inferred that serpentinization must have been involved the path of circulation beneath the DVF. Given the absence of ultramafic outcrops so far but keeping in mind that this area is still underexplored, source rocks subject to serpentinization might be olivine-rich gabbro or peridotite in the subsurface. A similar situation is found at the KHF along the Central Indian Ridge, where high H_2 concentrations measured in 2003 were initially taken as a signal of hydrothermal alteration of ultramafic assemblages and serpentinization, but olivine-rich gabbros were found about 15 km East of the KHF five years later (Gallant and Von Damm, 2006; Nakamura et al., 2008).

The high H_2 content in the Buddha’s Hands fluid indicates a strongly reducing setting at the DVF. It may play a major role on the distribution of REEs in the DVF fluids. The absolute concentrations and chondrite-normalized patterns of REE in the DVF fluids are comparable to those of hydrothermal fluids from other submarine hydrothermal systems (Fig. 8A). The enrichment of LREE over HREE is typical for the MOR systems and independent of the host rock composition (Allen and Seyfried, 2005).

During the water-rock interaction, HREE tend to be incorporated into the secondary alteration minerals, which enhances the LREE/HREE ratio in fluids (Beermann et al., 2017). Europium is redox sensitive and the Eu^{3+} can be reduced to Eu^{2+} under reducing condition. This behavior could result in decoupling of Eu from its REE neighbors during fluid circulation (Allen and Seyfried 2005; Tertre et al., 2008). As shown in Fig. 8B, the magnitude of positive Eu anomalies in DVF fluids is comparable to the mafic-hosted vent field TAG, but significantly higher compared to the other submarine hydrothermal systems. In addition, the large magnitude of the positive Eu anomaly is a characteristic fingerprint of ultramafic rock alteration, attributed to the strongly reducing conditions and intense water-rock interactions (Schmidt et al., 2007, 2011). An exception is the Rainbow field, whose Eu anomaly is interpreted to be the result of phase separation associated with strong reducing conditions. Formation of Cl-complexes increases the solubility of Eu (Douville et al., 2002). Thus, we interprete the extremely large Eu anomalies in the DVF samples as the combined effect from phase separation and water-rock interaction under strongly reducing conditions. The Eu^{2+} concentration is twice that of the REE^{3+} along the fluid pathway, as neighbouring trivalent REEs prefer partitioning into secondary alteration minerals (e.g. serpentine, tremolite). The higher positive Eu anomaly in the Buddha's Hands fluid than that in the A1 fluid could be related to phase separation.

5.4 A hybrid model for hydrothermal circulation at the Daxi Vent Field

The DVF is located on a small neo-volcanic ridge in an NTO setting. The only system with a comparable geological setting is at the Puy de Folles field located on the top of a large volcanic seamount within an NTO in the Northern Mid-Atlantic Ridge. A magma chamber is presumably the heat source to drive hydrothermal circulation at the Puy des Folles site (Cherkashov et al., 2010). Similarly, the presence of volcanos recognized from the bathymetric and basaltic lavas suggest the presence of a magmatic source beneath the DVF, although the location and size of the magma chamber is still unclear (Wang et al., 2021). The proposed involvement of serpentinization during hydrothermal circulation suggests that olivine-rich gabbros or abyssal peridotites must have been uplifted to shallower depth or possible deep reaching faults have penetrating into the lower crust or even to the upper mantle. Therefore, we propose that the hydrothermal processes at the DVF are controlled by tectonic and magmatic activities simultaneously. Here, we compare the geochemistry of hydrothermal fluids from the DVF with other hydrothermal systems hosted in a magmatic- or tectonic- controlled setting, respectively, to better understand the constraints on fluid evolution and material fluxes discharging into the oceans eventually.

The Rainbow field is located at the ultramafic footwall of a detachment fault with masses of seawater penetrating into the host rocks. The hydrothermal circulation at this site was proposed to be driven by an intrusive magmatic unit (Andreani et al., 2014). The Nibelungen field is located on a fault scarp east of the ridge axis. A deeply stored, old and degassed heat source, such as lower gabbroic cumulates, rather than active magmatic activity is deduced here (Schmidt et al., 2011). There is a prominent fault west of the field providing fluid pathways and uplifting the lower lithospheres, resulting in interactions between hydrothermal fluids with gabbroic rock, ultramafic rocks, and basaltic rocks successively. A hybrid model, with both mafic and ultramafic rocks being involved along the fluid pathway, is thus proposed for the DVF. The fundamental role of composition of rock substrates on the geochemistry of hydrothermal fluids is noticeable when comparing these three sites with each other (Table 6). The alteration of ultramafic rocks at the three sites left similar characteristic fingerprints, e.g. high concentrations of H_2 and CH_4, depletion of B compared to seawater, and a large positive Eu anomaly (Table 6; Fig. 5F; Fig. 7; Fig. 8B). However, concentrations of CH_4 and H_2 and the CH_4/H_2 ratio in the Nibelungen and Daxi fluids are lower than Rainbow and the Li/Cl ratios are higher. This is entirely consistent with the absence of serpentinization in basaltic rocks and their greater abundances of incompatible elements. Moreover, the relative low concentrations of CH_4 and H_2 in the brine phase fluid at the DVF can be also affected by phase separation because the dissolved gases will preferentially partition into the vapor phase, and will hence be depleted in the liquid phase (Von Damm, 1995).

The Cl content in the Buddha's Hands fluid is the highest among the hydrothermal fields at NTOs. It may be due to its great water depth and the increased of magma supply relative to other NTO sites. The DVF fluids are most similar to fluids from the Edmond field which is located on the wall of a rift valley at comparable water depth besides the ultramafic fingerprints (3300 m; Gallant and Von Damm, 2006). The hydrothermal circulation at the Edmond field was driven by a heat source that was relatively close to the surface and the phase separation was inferred to have occurred at 420-430 °C and 30-300 m below the seafloor. The similar compositions of hydrothermal fluids and p-T conditions of phase separation between the DVF and Edmond may be related to their similar circumstances, e.g. water depth and size and location of the heat source. The very high Cl content in fluids have also been observed from the Cleft segmen, JdFR (Table 6, Von Damm and Bischoff, 1987; Palmer and Edmond, 1989; Campbell and Edmond, 1989; Butterfield and Massoth, 1994). As most of the transition metals are transported as chlorocomplexes, the South Cleft with higher Cl contents have much higher metal contents. Although the North Cleft fluid have comparable Cl concentration with the Daxi and Edmond fluids, the Fe/Mn concentration is significantly lower while the major elements are still at high levels in the former. Combined with the relatively high Ca/Na ratio and low levels of H_2S, the low Fe suggests that the North Cleft fluid equilibrated at a relatively low temperature in the reaction zone. The Rainbow field also emanated phase-separated fluids. The concentrations of Br, alkalis, and alkali earth elements co-vary with Cl in these four fields. However, the higher Cl content did not result in higher metal concentrations, most metals are much higher in the Rainbow fluids (Table 6). The extremely high metal contents in Rainbow fluids, especially Fe which is two times higher than the Daxi and Edmond fluids, may be related not only to phase separation but also to the relatively low pH value. Whether the difference of lithology plays a certain role cannot be determined considering that there is no consistent difference in trace metal contents between ultramafic and mafic-hosted hydrothermal systems (Seyfried et al., 2004).

Precipitation of sulfide minerals in the subseafloor further differentiates the DVF fluids from those at Rainbow, Nibelungen, and Edmond whose endmember composition relates at high temperature reaction zones. Although the Rainbow fluids are strongly enriched in most of the transition and heavy metals, Cu is significantly higher in the Nibelungen fluid (Table 6). We interpret this a large proportion of initially mobilized Cu has been precipitated in the subseafloor (Seyfried et al., 2004). The temperatures of the DVF fluids are lowest and large portions of sulfide-forming elements, especially Cu, Co, Fe, were fixed in the sulfides, whereas Zn, Ag, Ga, Sb, and Cd were remobilized and enriched in the venting fluids (Table 6). By using the Edmond fluids as a reference, we calculate that 97% of Cu in Buddha's Hands fluid must have been fixed as Cu-sulfides and deposited in the subsurface. This seems an effective way to preserve metals leached from host rocks by forming metal sulfide deposits. The Von Damm field is another ultramafic-hosted hydrothermal system located on the Mount Dent oceanic core complex at 2350 m depth on the Mid-Cayman Rise (German et al., 2010). The Von Damm fluids are characterized by intermediate temperature (226 °C), low metal concentrations, intermediate pH (~5.56), and high Cl concentrations (651 mM, Table 6, McDermott, 2015; Hodgkinson et al., 2015). Although the Daxi and Von Damm fluids are similar in temperature and pH values, the characteristics of the latter can be attributed to the relatively lower temperatures of reaction due to its much shallower water depth. The temperature of water-rock interaction at the Daxi field should be much higher than the Von Damm. The intermediate temperature, low metal concentrations, and intermediate pH of the Daxi fluids are mainly due to mixing with entrained seawater, while its Fe concentration is still significant high due to limited precipatation. In summary, we provided a hybrid model of hydrothermal circulation controlled by tectonic and magmatic activities simultaneously at the NTO to understand the unique geochemical characteristics of the DVF fluids (Fig. 9).

6. Summary and conclusion

The Daxi Vent Field is unique because it is located on the volcanic ridge within an NTO on the Carlsberg Ridge. The presence of normal faults on both flanks of the neo-volcanic ridge and the magmatic activities facilitates the development of hydrothermal circulation. For the first time, we report the chemistry of vent fluids from two locations of the DVF, Buddha's Hands and A1. A striking feature of their vent fluid chemistry is the unusually high Cl concentration in Buddha's Hands fluid (928 mM) and the low Cl concentration in the A1 fluid (303 mM) in close proximity. The alkalis (Na, K, Li, and Rb) co-vary with Cl with similar ratios between the Buddha's Hands and A1 sites. This suggests that they have been subjected to phase separation and share a common source at depth. The segregated vapor and brine phases have been re-mixed in variable proportions during their ascent.

Furthermore, the fluid samples are characterized by a depletion of B, enrichment of Ca, and extremely large Eu anomalies, at similar temperatures 273 and 272 °C, respectively. The dissolved gases H_2 and CH_4 are strongly enriched in the Buddha's Hands fluid. The geochemical signature suggests that serpentinization has been involved along the ascent pathway during circulation. Olivine-rich gabbro or abyssal peridotite must have been uplifted to shallow depth or deep reaching faults have penetrated into the lower crust or even the upper mantle. Due to the open hydrologic regime beneath the DVF, large amounts of cold seawater must have been entrained into the discharge zone and mixed with ascending hot fluids. The fluid temperature dereased from 430 °C to 270 °C and hence large amounts of sulfide minerals may have been deposited in the subsurface. This caused depletion of sulfide-forming elements (Cu, Co, Fe) and enrichment of Zn, Ag, Ga, Sn, Sb, and Cd in the venting fluids. We suggest that Cu-rich massive sulfide deposits may be found in the subsurface at DVF. A hybrid model is proposed for hydrothermal circulation at the DVF that is different from typical tectonic or magmatic controlled hydrothermal fields elsewhere. The DVF fluid samples provide an opportunity to extend our understanding of systems at NTOs. It not only broadens our understanding, but also provides new and supplementary information for eventual estimating mass and heat fluxes from hydrothermal fields to the ocean and the formation of seafloor massive sulfide deposits.

Data availability:

Datasets related to this article can be found at https://dx.doi.org/10.17632/gc2mpw74z8.1

Acknowledgements：

This study was supported by the National Key Research and Development Program of China (2021YFF0501304), National Natural Science Foundation of China (No. 91951201, 41976076, 41976075), Scientific Research Fund of the Second Institute of Oceanography, MNR (grant number JZ1901), China Ocean Mineral Resources R&D Association project (DY135-S2-1), and the Talent Program of Zhejiang Province (grant no. 2018R51003). We are grateful to the HOV *Jiaolong* operations team, the scientific parties, and crews of the R/V *Xiangyanghong* 9 for their support and cooperation. We also thank Bettina Domeyer, Ulrike Westernströer, Verena Heinath, and Karen Bremer for their help with analytical work.

Author Contributions：

X.H., Y.W. and Z.Q. designed the research project; X.W. and Z.Z. processed the samples onboard; X.W., X.H., D.G.-S., M.S. and T.Z. performed the data analysis. X.W., X.H., Y.W., D.G.-S., M.S., Z.Q., T.Z., P.Z., X.Y., J.L. and H.L carried out the data interpretation. X.W. and X.H led the writing of the manuscript with input from all authors.

References

Allen, D.E., Seyfried Jr, W.E., 2005. REE controls in ultramafic hosted MOR hydrothermal systems: An experimental study at elevated temperature and pressure. Geochimica et Cosmochimica Acta. 69(3), 675-683. https://doi.org/10.1016/j.gca.2004.07.016

Agranier, A., Lee, C.-T.A., Li, Z.-X.A., Leeman, W.P., 2007. Fluid-mobile element budgets in serpentinized oceanic lithospheric mantle: insights from B, As, Li, Pb, PGEs and Os isotopes in the Feather River Ophiolite, California. Chemical Geology. 245, 230–241. https://doi.org/10.1016/j.chemgeo.2007.08.008

Andreani, M., Escartin, J., Delacour, A., Ildefonse, B., Godard, M., Dyment, J., Fallick, A.E., Fouquet, Y., 2014. Tectonic structure, lithology, and hydrothermal signature of the Rainbow massif (Mid-Atlantic Ridge 36°14′N). Geochemistry, Geophysics, Geosystems. 15, 3543-3571. https://doi.org/10.1002/2014GC005269

Bach, W., Roberts, S., Vanko, D.A., Binns, R.A., Yeats, C.J., Craddock, P.R., Humphris, S.E., 2003. Controls of fluid chemistry and complexation on rare-earth element contents of anhydrite from the Pacmanus subseafloor hydrothermal system, Manus Basin, Papua New Guinea. Miner. Deposita. 38, 916-935. https://doi.org/10.1007/s00126-002-0325-0

Badullovich, N., Moynier, F., Creech, J., Teng, F., Sossi, P.A., 2017. Tin isotopic fractionation during igneous differentiation and Earch's mantle composition. Geochemical Perspectives Letters. 5, 24-28. https://doi.org/10.7185/geochemlet.1741

Baker, .ET., German, C.R., 2004. On the global distribution of hydrothermal vent fields. In German, C.R., Lin, J., Parson, L.M (Eds.), Mid-Ocean Ridges: Hydrothermal Interactions Between the Lithosphere and Oceans. American Geophysical Union, Washington, DC, pp. 245–267. https://doi.org/10.1029/148GM10

Beaulieu, S.E., Szafrański, K.M., 2020. InterRidge Global Database of Active Submarine Hydrothermal Vent Fields Version 3.4. PANGAEA. https://doi.org/10.1594/PANGAEA.917894

Beermann, O., Garbe-Schönberg, D., Bach, W., Holzheid, A., Holzheid, A., 2017. Time-Resolved Interaction of Seawater with Gabbro: An Experimental Study of Rare-Earth Element Behavior up to 475 °C, 100MPa. Geochimica et Cosmochimica Acta. 197, 167-192. https://doi.org/10.1016/j.gca.2016.10.016

Berndt, M.E., Allen, D.E., Seyfried Jr, W.E., 1996. Reduction of CO_2 during serpentinization of olivine at 300 °C and 500 bar. Geology. 24, 351-354. https://doi.org/10.1130/0091-7613(1996)024<0351:ROCDSO>2.3.CO;2

Berndt, M.E., Seyfried Jr, W.E., 1990. Calibration of Br/Cl fractionation during subcritical phase separation of seawater: Possible halite at 9 to 10°N East Pacific Rise. Geochimica et Cosmochimica Acta. 61, 2849-2854. https://doi.org/10.1016/S0016-7037(97)00134-8

Berndt, M.E., Seyfried Jr, W.E., 1993. Calcium and sodium exchange during hydrothermal alteration of calcic plagioclase at 400 °C and 400 bars. Geochimica et Cosmochimica Acta. 57(18), 4445-4451. https://doi.org/10.1016/0016-7037(93)90494-H

Bischoff, J. L., Rosenbauer, R. J., 1985. An empirical equation of state for hydrothermal seawater (3.2 percent NaCl). American Journal of Science. 285(8), 725-763. https://doi.org/ 10.2475/ajs.285.8.725

Bischoff, J. L., Pitzer, K. S., 1989. Liquid-Vapor Relations for the System NaCl-H_2O: Summary of the P-T- x Surface from 300° to 500 °C. American Journal of Science. 289(3), 217–48. https://doi.org/10.2475/ajs.289.3.217

Boschi, C., Dini, A., Früh-Green, G., Kelley, D., 2008. Isotopic and element exchange during serpentinization and metasomatism at the Atlantis Massif (MAR 30°N): Insights from B and Sr isotope data. Geochimica Et Cosmochimica Acta. 72(7), 1801-1823. https://doi.org/10.1016/j.gca.2008.01.013

Butterfield, D.A., Massoth, G.J., 1994. Geochemistry of North Cleft Segment vent field: Temporal changes in chlorinity and their possible relation to recent volcanism. Journal of Geophysical Research. 99, 4951-4968. https://doi.org/10.1029/93jb02798

Campbell, A.C., Edmond, J.M., 1989. Halide systematics of submarine hydrothermal vents. Nature. 342, 168-170. https://doi.org/10.1038/342168a0

Charlou, J.L., Donval, J.P., Fouquet, Y., Jean-Baptiste, P., Holm, N.G., 2002. Geochemistry of high H_2 and CH_4 vent fluids issuing from ultramafic rocks at the rainbow hydrothermal field (36°14'N, MAR). Chemical Geology. 191(4), 345-359. https://doi.org/10.1016/S0009-2541(02)00134-1

Charlou, J.L., Donval, J.P., Douville, E., Jean-Baptiste, P., Radford-Knoery, J., Fouquet, Y., Dapoigny, A., Stievenard, M., 2000. Compared geochemical signatures and the evolution of Menez Gwen (35°50′N) and Lucky Strike (37°17′N) hydrothermal fluids, South of the Azores Triple Junction on the Mid-Atlantic

Ridge. Chemical Geology. 171(1-2), 49–75. https://doi.org/10.1016/S0009-2541(00)00244-8

Charlou, J.L., Donval, J.P., Jean-Baptiste, P., Dapoigny, A., Rona, P.A., 1996. Gases and helium isotopes in high temperature solutions sampled before and after ODP Leg 158 drilling at TAG hydrothermal field (26°N, MAR). Geophysical Research Letters. 23(23), 3491-3494. https://doi.org/10.1029/96GL02141

Charlou, J.L., Donval, J.P., Konn, C., Ondreas, H., Fouquet, Y., JeanBaptiste, P., Fourré, E., 2010. High production and fluxes of H_2 and CH_4 and evidence of abiotic hydrocarbon synthesis by serpentinization in ultramafic-hosted hydrothermal systems on the Mid-Atlantic Ridge. In: Rona, P.A., Devey, C. W., Dyment, J., Murton, B. J. (Eds.), Diversity of Hydrothermal Systems on Slow Spreading Ocean Ridges. American Geophysical Union, Washington, DC, pp. 265-296. https://doi.org/ 10.1029/2008GM000752

Chavagnac, V, Leleu, T., Fontaine, F., Cannat, M., Ceuleneer, G., Castillo, A., 2018. Spatial variations in vent chemistry at the Lucky Strike Hydrothermal Field, Mid-Atlantic Ridge (37°N): Updates for subseafloor flow geometry from the newly discovered Capelinhos Vent. Geochemistry, Geophysics, Geosystems. 19. https://doi.org/ 10.1029/2018GC007765

Cherkashov, G., Poroshina, I., Stepanova, T., Ivanov, V., Bel'Tenev, V., Lazareva, L., Rozhdestvenskaya, I., Samovarov, M., Shilov, V., Glasby, G.P., Fouquet, Y., Kuznetsov, V., 2010. Seafloor massive sulfides from the northern equatorial Mid-Atlantic Ridge: New discoveries and perspectives. Marine Georesources and Geotechnology. 28(3), 222-239. https://doi.org/10.1080/1064119X.2010.483308

Dias, Á.S., Barriga, F.J.A.S., 2006. Mineralogy and geochemistry of hydrothermal sediments from the serpentinite-hosted Saldanha hydrothermal field (36°34′N;

33°26′W) at MAR. Marine Geology. 225(1–4), 157-175. http://dx.doi.org/10.1016/j.margeo.2005.07.013

de Ronde, C.E., Stucker, V.K., 2015. Seafloor hydrothermal venting at volcanic arcs and backarcs. The Encyclopedia of Volcanoes (Second Edition). 823-849. https://doi.org/10.1016/B978-0-12-385938-9.00047-X

Douville, E., Bienvenu, P., Charlou, J.L. , Donval, J. P., Fouquet, Y., Appriou, P., Gamo, T., 1999. Yttrium and rare earth elements in fluids from various deep-sea hydrothermal systems. Geochimica et Cosmochimica Acta. 63(5), 627-643. https://doi.org/10.1016/S0016-7037(99)00024-1

Douville, E., Charlou, J.L., Oelkers, E.H., Bienvenu, P., Jove Colon, C.F., Donval, J.P., Fouquet, Y., Prieur, D., Appriou, P., 2002. The Rainbow Vent Fluids (36°14′N, MAR): The influence of ultramafic rocks and phase separation on trace metal content in Mid-Atlantic Ridge hydrothermal fluids. Chemical Geology. 184(1–2), 37–48. https://doi.org/10.1016/S0009-2541(01)00351-5

Driesner, T., Herinrich, C.A., 2007. The system H_2O-NaCl. Part I: correlation formulae for phase relations in temperature–pressure–composition space from 0 to 1000 ℃, 0 to 5000 bar, and 0 to 1 XNaCl. Geochim. Cosmochim. Acta. 71, 4880–4901. https://doi.org/10.1016/j.gca.2006.01.033

Edmonds, H.N., 2010. Chemical signatures from hydrothermal venting on slow spreading ridges. In: Rona, P.A., Devey, C.W., Dyment, J., Murton, B.J. (Eds.), Diversity of Hydrothermal Systems on Slow Spreading Ocean Ridges. American Geophysical Union, Washington, DC, pp. 27–42. https://doi.org/10.1029/2010GM000931

Edmond, J.M., Measures, C., McDuff, R.E., Chan, L.H., Collier, R., Gordon, L.I., Corliss, J.B., 1979. Ridge crest hydrothermal activity and the balances of the major and minor elements in the ocean: The Galapagos data. Earth and Planetary Science Letters. 46(1), 1-18. https://doi.org/10.1016/0012-821X(79)90061-X

Evensen, N.M., Hamilton, P.J., O'Nions, R.K., 1978. Rare-earth abundances in chondritic meteorites. Geochimica Et Cosmochimica Acta. 42(8), 1199-1212. https://doi.org/10.1016/0016-7037(78)90114-X

Foustoukos, D.I., Seyfried Jr, W.E., 2007. Quartz solubility in the two-phase and critical region of the NaCl–KCl–H_2O System: Implications for submarine hydrothermal vent systems at 9°50′N East Pacific Rise. Geochimica et Cosmochimica Acta. 71(1), 186–201. https://doi.org/10.1016/j.gca.2006.08.038

Fouquet, Y., Pierre, C., Etoubleau, J., Charlou, J.L., Ondréas, H., Barriga, F.J.A.S., Cherkashov, G., Semkova, T., Poroshina, I., Bohn, M., Donval, J.P., Henry, K., Murphy, P.J., Rouxel, O., 2010. Geodiversity of hydrothermal along the Mid-Atlantic Ridge and ultramafic-hosted mineralization: A new type of oceanic Cu-Zn-Co-Au Volcanogenic Massive Sulfide Deposit. In: Rona, P.A., Devey, C.W., Dyment, J., Murton, B.J. (Eds.), Diversity of Hydrothermal Systems on Slow Spreading Ocean Ridges. AGU, Washington, D.C., pp. 321-367. https://doi.org/10.1029/2008GM00074

Fujii, M., Okino, K., Sato, T., Sato, H., Nakamura, K., 2016. Origin of magnetic highs at ultramafic hosted hydrothermal systems: Insights from the Yokoniwa site of Central Indian Ridge. Earth and Planetary Science Letters. 441, 26-37. https://doi.org/10.1016/j.epsl.2016.02.018

Gallant, R.M., Von Damm, K.L., 2006. Geochemical controls on hydrothermal fluids from the Kairei and Edmond vent fields, 23°-25°S, Central Indian Ridge.

Geochemistry, Geophysics, Geosystems. 7(6), Q06018. https://doi.org/10.1029/2005GC001067

Gamo, T., Chiba, H., Yamanaka, T., Okudaira, T., Hashimoto, J., Tsuchida, S., Ishibashi, J., Kataoka, S., Tsunogai, U., Okamura, K., Sano, Y., Shinjo, R., 2001. Chemical characteristics of newly discovered black smoker fluids and associated hydrothermal plumes at the Rodriguez Triple Junction, Central Indian Ridge. Earth and Planetary Science Letters. 193(3-4), 371-379. https://doi.org/10.1016/S0012-821X(01)00511-8

Gena, K., Kase, K., Chiba, H., Nakashima, K., 2005. Tin-bearing chalcopyrite and platinum-bearing bismuthinite in the active Tiger sulfide chimney, Yonaguni Knoll IV seafloor hydrothermal system, Okinawa Trough, Japan. American Geophysical Union, Fall Meeting 2005, abstract #V51C-1492.

German, C.R., Seyfried Jr, W.E., 2014. Hydrothermal Processes. In: H. D. Holland and K. K. Turekian. (Eds.), Treatise on Geochemistry (Second Edition), Vol. 8, The Oceans and Marine Geochemistry. Elsevier, Oxford, pp. 191-233. http://dx.doi.org/10.1016/B978-0-08-095975-7.00607-0.

German, C.R., Bowen, A., Coleman, M.L., Honig, D.L., Huber, J.A., Jakuba, M.V., Kinsey, J.C., Kurz, M.D., Leroy, S., McDermott, J.M., Lépinay, B.M., Nakamura, K., Seewald, J.S., Smith, J.L., Sylva, S.P., Van Dover, C.L., Whitcomb, L.L., Yoerger, D.R., 2010. Diverse styles of submarine venting on the ultraslow spreading Mid-Cayman Rise. Proceedings of the National Academy of Sciences, 107 (32), 14020-14025. http://dx.doi.org/10.1073/pnas.1009205107

Gràcia, E., Bideau, D., Hekinian, R., Lagabrielle, Y., Parson, L.M., 1997. Along-axis magmatic oscillations and exposure of ultramafic rocks in a second-order segment of the Mid-Atlantic Ridge (33°43'N to 34°07'N). Geology. 25(12), 1059. http://doi.org/10.1130/0091-7613(1997)025<1059:AAMOAE>2.3.CO;2

Gràcia, E., Charlou, J.L., Radford-Knoery, J., Parson, L.M., 2000. Non-transform offsets along the mid-atlantic ridge south of the azores (38°N–34°N): Ultramafic exposures and hosting of hydrothermal vents. Earth and Planetary Science Letters. 177(1-2), 89-103. http://doi.org/10.1016/s0012-821x(00)00034-0

Grozeva, N.G., Klein, F., Seewald, J.S., Sylva, S.P., 2020. Chemical and isotopic analyses of hydrocarbon-bearing fluid inclusions in olivine-rich rocks. Philosophical Transactions of the Royal Society A. 378, 20180431. http://doi.org/10.1098/rsta.2018.0431

Hannington, M.D., de Ronde, C.E.J., Petersen, S., 2005. Sea-floor tectonics and submarine hydrothermal systems. In: Hedenquist, J.W., Thompson, J.F.H., Goldfarb, R.J., Richards, J.P. (Eds.), Economic Geology 100th Anniversary Volume. Society of Economic Geologists, Inc. pp. 111-141. https://doi.org/10.5382/AV100.06

Hodgkinson, M.R.S., Webber, A.P., Roberts, S., Mills, R.A., Connelly, D.P., Murton, B.J., 2015. Talc-dominated seafloor deposits reveal a new class of hydrothermal system. Nature Communications. 6, 10150. https://doi.org/10.1038/ncomms10150

Horita, J., Berndt, M.E., 1999. Abiogenic methane formation and isotope fractionation under hydrothermal conditions. Science, 285, 1055-1057. https://doi.org/10.1126/science.285.5430.1055

James, R.H., Green, D.R.H., Stock, M.J., Alker, B.J., Banerjee, N.R., Cole, C., German, C.R., Huvenne, V.A.I., Powell, A.M., Connelly, D.P., 2014. Composition of hydrothermal fluids and mineralogy of associated chimney material on the East Scotia Ridge back-arc spreading centre, Geochimica et Cosmochimica Acta. http://dx.doi.org/10.1016/j.gca.2014.04.024

Jochum, K.P., Hofmann, A.W., Seufert, H.M., 1993. Tin in mantle-derived rocks: constraints on earth evolution. Geochimica et Cosmochimica Acta. 57(15), 3585-3595. https://doi.org/10.1016/0016-7037(93)90141-I

Keith, M., Haase, K.M., Schwarz-Schampera, U., Klemd, R., Petersen, S., Bach, W., 2014. Effects of temperature, sulfur, and oxygen fugacity on the composition of sphalerite from submarine hydrothermal vents. Geology. 42, 699–702. https://doi.org/10.1016/j.oregeorev.2015.07.012

Klein, F., Grozeva, N.G., Seewald, J.S., 2019. Abiotic methane synthesis and serpentinization in olivine-hosted fluid inclusions. Proceedings of the National Academy of Sciences. 116 (36), 17666-17672. https://doi.org/10.1073/pnas.1907871116

Klein, F., Grozeva, N.G., Seewald, J.S., McCollom, T.M., Humphris, S.E., 2015. Experimental constraints on fluid-rock reactions during incipient serpentinization of harzburgite. American Mineralogist. 100, 991-1002. https://doi.org/10.2138/am-2015-5112

Kumagai, H., Nakamura, K., Toki, T., Morishita, T., Okino, K., Ishibashi, J.I., Tsunogai, U., Kawagucci, S., Gamo, T., Shibuya, T., Sawaguchi, T., Neo, N., Joshima, M., Sato, T., Takai, K., 2008. Geological background of the Kairei and Edmond hydrothermal fields along the Central Indian Ridge: Implications of their vent fluids' distinct chemistry. Geofluids. 8(4), 239-251. https://doi.org/10.1111/j.1468-8123.2008.00223.x

Lartaud, F., de Rafelis, M., Oliver, G., Krylova, E., Dyment, J., Ildefonse, B., Thibaud, R., Gente, P., Hoisé, E., Meistertzheim, A-L., Fouquet, Y., Gaill, F., Le Bris, N., 2010. Fossil clams from a serpentinite-hosted sedimented vent field near the active smoker complex Rainbow, MAR, 36°13'N: Insight into the biogeography of vent fauna. Geochemistry, Geophysics, Geosystems. 11(8), Q1A. https://doi.org/10.1029/2010GC003079

Lartaud, F., Little, C.T.S., de Rafelis, M., Bayon, G., Dyment, J., Ildefonse, B., Gressier, V., Fouquet, Y., Gaill, F., Le Bris, N., 2011. Fossil evidence for serpentinization fluids fueling chemosynthetic assemblages. Proceedings of the National Academy of Sciences. 108(19), 7698–7703. http://doi.org/10.1073/pnas.1009383108

Li, B., Shi, X., Wang, J., Yan, Q., Liu, C., 2018. Tectonic environments and local geologic controls of potential hydrothermal fields along the Southern Mid-Atlantic Ridge (12–14°S). Journal of Marine Systems. 181, 1-13. https://doi.org/10.1016/j.jmarsys.2018.02.003

Lilley, M.D., Butterfield, D.A., Lupton, J.E., Olson, E.J., 2003. Magmatic events can produce rapid changes in hydrothermal vent chemistry. Nature. 422, 878-881. https://doi.org/10.1038/nature01569

McCaig, A.M., Delacour, A., Fallick, A.E., Castelain, T., FRüh-Green, G., 2010. Detachment fault control on hydrothermal circulation systems: Interpreting the subsurface beneath the TAG Hydrothermal Field using the isotopic and geological evolution of oceanic core complexes in the Atlantic. In: Rona, P.A., Devey, C. W., Dyment, J., Murton, B. J. (Eds.), Diversity of Hydrothermal Systems on Slow Spreading Ocean Ridges. American Geophysical Union, Washington, DC, pp. 207-239. https://doi.org/ 10.1029/2008GM000729

McCollom, T.M., Seewald, J.S., 2001. A reassessment of the potential for reduction of dissloved CO2 to hydrocarbons during serpentinization of olivine. Geochimica et Cosmochimica Acta. 65, 3769-3778. https://doi.org/10.1016/S0016-7037(01)00655-X

McDermott, J.M. 2015. Geochemistry of deep-sea hydrothermal vent fluids from the Mid-Cayman Rise, Caribbean Sea. Massachusetts Institute of Technology, Department of Earth, Atmospheric, and Planetary Sciences; and the Woods Hole Oceanographic Institution (D). http://hdl.handle.net/1721.1/97337

Mottl, M.J., 2012. VentDB: EPR21N. Mid-Ocean Ridge Hydrothermal Vent Chemistry Data Collection. https://doi.org/10.1594/IEDA/100208

Mottl, M.J., Holland, H.D., 1978. Chemical exchange during hydrothermal alteration of basalt by seawater-I. Experimental results for major and minor components of seawater. Geochimica et Cosmochimica Acta. 42(8), 1103-1115. https://doi.org/10.1016/0016-7037(78)90107-2

Mottl, M. J., Holland, H.D., Corr, R.F., 1979. Chemical exchange during hydrothermal alteration of basalt by seawater—II. Experimental results for Fe, Mn, and sulfur species. Geochimica et Cosmochimica Acta. 43(6), 869-884. https://doi.org/10.1016/0016-7037(79)90225-4

Nakamura, K., Morishita, T., Takai, K., Hara, K., Kumagai, H., 2008. Serpentinized olivine-rich gabbros near the kairei hydrothermal field central indian ridge: a key to understanding the unique chemistry of the vent fluid. Geochmica Et Cosmochimica Acta. 72(12), A670.

Oosting, S.E. and Von Damm, K.K. 1996. Bromide/chloride fractionation in seafloor hydrothermal fluids from 9-10°N East Pacific Rise. Earth and Planetary Science Letters. 144, 133-145. https://doi.org/10.1016/0012-821X(96)00149-5

Palmer, M.R., Edmond, J.M., 1989. Cesium and rubidium in submarine hydrothermal fluids: evidence for recycling of alkali elements. Earth and Planetary Science Letters. 95. 8-14. https://doi.org/10.1016/0012-821X(89)90163-5

Paulick, H., Bach, W., 2006. Phyllosilicate alteration mineral assemblages in the active subseafloor Pacmanus Hydrothermal System, Papua New Guinea, ODP Leg 193. Econ. Geol. 101(3), 633-650. https://doi.org/10.2113/gsecongeo.101.3.633

Pester, N.J., Ding, K., Seyfried Jr, W.E., 2014. Magmatic Eruptions and Iron Volatility in Deep-Sea Hydrothermal Fluids. Geology. 42(3), 255-258. https://doi.org/10.1130/G35079.1

Pester, N.J., Rough, M., Ding, K., Seyfried Jr, W.E., 2011. A new Fe/Mn geothermometer for hydrothermal systems: implications for high-salinity fluids at 13°N on the East Racific rise. Geochimica et Cosmochimica Acta. 75(24), 7881-7892. https://doi.org/10.1016/j.gca.2011.08.043

Rosenbauer, R.J., Bischoff, J.L., 1983. Uptake and transport of heavy metals by heated seawater: A summary of the experimental results. In: Rona, P.A., Boström, K., Laubier, L., Smith, K.L. (Eds.), Hydrothermal Processes at Seafloor Spreading Centers. NATO Conference Series. vol IV, no. 12, pp. 177-197. Plenum press. https://doi.org/10.1007/978-1-4899-0402-7_9

Schmidt, K., Garbe-Schönberg, D., Hannington, M.D., Anderson, M.O., Bühring, B., Haase, K., Haruel, C., Lupton, J., Koschinsky, A., 2017. Boiling vapour-type fluids from the Nifonea vent field (New Hebrides Back-Arc, Vanuatu, SW Pacific): Geochemistry of an early-stage, post-eruptive hydrothermal system. Geochimica et Cosmochimica Acta. 207, 185-209. https://doi.org/10.1016/j.gca.2017.03.016

Schmidt, K., Garbe-Schönberg, D., Koschinsky, A., Strauss, H., Jost, C.L., Klevenz, V., Königer, P., 2011. Fluid elemental and stable isotope composition of the Nibelungen hydrothermal field (8°18′s, Mid-Atlantic Ridge): constraints on fluid–rock interaction in heterogeneous lithosphere. Chemical Geology. 280(1-2), 1-18. https://doi.org/10.1016/j.chemgeo.2010.07.008

Schmidt, K., Koschinsky, A., Garbe-Schönberg, D., de Carvalho L.M., Seifert, R., 2007. Geochemistry of hydrothermal fluids from the ultramafic-hosted Logatchev hydrothermal field, 15°N on the Mid-Atlantic Ridge: Temporal and spatial investigation. Chemical Geology. 242(1–2), 1–21. https://doi.org/10.1016/j.chemgeo.2007.01.023

Seewald, J.S., Seyfried Jr, W.E., 1990. The effect of temperature on metal mobility in subseafloor hydrothermal systems: constraints from basalt alteration experiments. Earth and Planetary Science Letters. 101(2–4), 388–403. https://doi.org/10.1016/0012-821x(90)90168-w

Seyfried Jr, W.E., 2003. Chemistry of hydrothermal vent fluids from the Main Endeavour Field, northern Juan de Fuca Ridge: Geochemical controls in the aftermath of June 1999 seismic events. Journal of Geophysical Research: Solid Earth. 108(B9), 2429. https://doi.org/10.1029/2002JB001957

Seyfried, W.E., Foustoukos, D.I., Allen, D.E., 2004. Ultramafic-hosted hydrothermal systems at mid-ocean ridges: chemical and physical controls on pH, redox and carbon reduction reactions. In: German, C., Lin, J. (Eds.), Mid-Ocean Ridges: Hydrothermal Interactions between the Lithosphere and Oceans. American Geophysical Union, Washington, DC, pp. 267–284. https://doi.org/10.1029/148GM11

Seyfried Jr, W.E., Janecky, D.R., Mottl, M.J., 1984. Alteration of the oceanic crust: implications for geochemical cycles of lithium and boron. Geochimica et Cosmochimica Acta. 48(3), 557-569. https://doi.org/10.1016/0016-7037(84)90284-9

Seyfried Jr, W.E., Pester, N.J., Ding, K., Rough, M., 2011. Vent fluid chemistry of the Rainbow hydrothermal system (36°N, MAR): Phase equilibria and in situ Ph controls on subseafloor alteration processes. Geochimica et Cosmochimica Acta. 75(6), 1574–1593. https://doi.org/10.1016/j.gca.2011.01.001

Sleep, N.H., Morton, J.L., 1983. Heat loss and clogging beneath black smoker vents. Eos. 64, 724

Tao, C. , Seyfried Jr, W.E. , Lowell, R.P. , Liu, Y. , Liang, J., Guo, Z., Ding, K., Zhang, H., Liu, L., Egorov, I., Liao, S., Zhao, M., Zhou, J., Deng, X., Li, H., Wang, H., Cai, W., Zhang, G., Zhou, H., Lin, J., Li, W., 2020. Deep high-temperature hydrothermal circulation in a detachment faulting system on the ultra-slow spreading ridge. Nature Communications. 11(1). https://doi.org/10.1038/s41467-020-15062-w

Tertre, E., Hofmann, A., Berger, G., 2008. Rare earth element sorption by basaltic rock: experimental data and modeling results using the "generalised composite approach". Geochimica et Cosmochimica Acta. 72(4), 1043-1056. https://doi.org/10.1016/j.gca.2007.12.015

Tivey, M.K., 2007. Generation of seafloor hydrothermal vent fluids and associated mineral deposits. oceanography. 20(1), 50–65. https://doi.org/10.5670/oceanog.2007.80

Tivey, M.K., Humphris, S.E., Thompson, G., Hannington, M.D., Rona, P.A., 1995. Deducing patterns of fluid flow and mixing within the tag active hydrothermal mound using mineralogical and geochemical data. Journal of Geophysical Research Atmosphere. 100, 12527-12555. https://doi.org/10.1029/95JB00610

Von Damm, K.L., Edmond, J.M., Measures, C.I., Grant, B., 1985. Chemistry of submarine hydrothermal solutions at Guaymas Basin, Gulf of California. Geochim. Cosmochim. Acta. 49, 2221-2237. http://doi.org/10.1016/0016-7037(85)90223-6

Von Damm, K.L. 1990. Seafloor Hydrothermal Activity: Black Smoker Chemistry and Chimneys. Annual Review of Earth and Planetary Sciences. 18, 173–204. https://doi.org/10.1146/annurev.ea.18.050190.001133

Von Damm, K.L., 1995. Controls on the chemistry and temporal variability of seafloor hydrothermal fluids, seafloor hydrothermal systems. In: Humphris, S. E., Zierenberg, R. A., Mullineaux, L. S. and Thomson, R. E. (Eds.), Seafloor Hydrothermal Systems: Physical, Chemical, Biological, and Geological Interactions, vol. 91. AGU Monograph. American Geophysical Union, pp. 222–247. https://doi.org/10.1029/GM091p0222

Von Damm, K.L., Bischoff, J.L., 1987. Chemistry of hydrothermal solutions from the Southern Juan de Fuca Ridge. Journal of Geophysical Research. 92 (B11), 11334-11346. https://doi.org/10.1029/JB092iB11p11334

Von Damm, K.L., Bray, A.M., Buttermore, L.G., Oosting, S.E., 1998. The geochemical controls on vent fluids from the Lucky Strike vent field, Mid-Atlantic Ridge. Earth and Planetary Science Letters. 160(3-4), 521-536. https://doi.org/10.1016/S0012-821X(98)00108-3

Wang, Y., Han, X., Zhou, Y., Qiu, Z., Yu, X., Petersen, S., Li, H., Yang, M., Chen, Y., Liu, J., Wu, X., Luo, H., DY33, DY38 Leg 1 Shipboard Scientific Party.,2021. The Daxi Vent Field: An active mafic-hosted hydrothermal system at a non-transform offset on the slow-spreading Carlsberg Ridge, 6°48′N. Ore Geology Reviews. http://doi.org/10.1016/j.oregeorev.2020.103888.

Webber, A.P., Roberts, S., Murton, B.J., Hodgkinson, M.R.S., 2015. Geology, sulfide geochemistry and supercritical venting at the Beebe hydrothermal vent field, Cayman Trough. Geochemistry, Geophysics, Geosystems. 16, 2661-2678. https://doi.org/10.1002/2015GC005879

Wu, S.J., Yang, C.J., Huang, H.C., 2014. Development of an electric control gas-tight sampler for seafloor hydrothermal fluids. Journal of Zhejiang University Science A. 15(2), 120–129. https://doi.org/10.1631/jzus.A1300233

Zhang, Z., 2020. Rapid shifts in chemical and isotopic compositions of sediment pore waters in the Amami Sankaku Basin in response to initial arc rifting in the mid-Oligocene. Geochemistry, Geophysics, Geosystems. 21 (3), 117. https://doi.org/10.1029/2019GC008845.

Zong, T., Han, X., Liu, J., Wang, Y., Qiu, Z., Li. H., Yu, X., 2019. H_2O in basaltic glasses from the slow-spreading Carlsberg Ridge: Implications for mantle source and magmatic processes. Lithos. 332-333, 274-286. https://doi.org/10.1016/j.lithos.2019.01.022

Figures and tables

Table 1: Information on the fluid samples.

Vent site	Water depth (m)	Latitude/longitude	Sample ID	Temperature (°C)	pH
Buddha's Hands	3453	6°48′07″N/60°10′26″E	38I-DIVE06-JL128-B-CY	273	5.25
A1	3452	6° 48′07″N/60°10′30″E	38I-DIVE06-JL128-C-CY	272	6.74

Table 2: Measured and calculated end-member (EM) compositions of vent fluids collected at the chimney orifices of Buddha's Hands and A1. Gas content of seawater are from Charlou et al., 2002. bdl = below detection limit, nd = not determined.

	Buddha's Hands		A1		Seawater
	Measured	EM	Measured	EM	
Mg, mM	27.5	0	44.3	0	52.6
SO_4, mM	11.8	-5.88	22.3	-8.22	28.2
CO_2, mM	1.74	1.12	nd	nd	2.30
CH_4, mM	0.422	0.884	nd	nd	0.0003
H_2, mM	3.37	7.07	nd	nd	0.0004
H_2S, mM	bdl	bdl	nd	nd	0
Cl, mM	726	928	504	303	542
Br, μM	1135	1466	758	354	833
B, μM	407	411	356	98.4	404
Si, mM	0.602	1.17	0.289	1.39	0.0850
Al, μM	0.415	0.869	bdl	bdl	bdl
Na, mM	599	744	432	245	467
K, mM	21.8	34.7	10.2	10.9	10.0
Ca, mM	39.2	71	12.4	24.2	10.2
Li, μM	399	807	60.6	245	26.2
Rb, μM	10.4	20.5	2.06	6.28	1.27
Cs, nM	52.5	105	12.4	66.1	2.25
Sr, μM	142	203	80.6	33.7	89.5
Fe, μM	5690	11,916	57.7	365	0.0291
Mn, μM	737	1550	87.0	564	bdl
Cu, μM	1.62	3.39	0.251	1.59	bdl
Zn, μM	13.5	28.2	31.4	199	0.0188
Cd, nM	19.0	39.7	35.4	224	bdl
Ba, μM	2.69	5.53	1.31	7.79	0.0897
Co, μM	0.588	1.23	0.0932	0.590	bdl
Pb, nM	38.1	70.8	5.45	34.5	bdl
Ag, nM	6.04	12.7	8.28	52.4	bdl
Sb, nM	1.57	1.20	4.55	18.6	1.91
Tl, nM	2.18	4.52	1.31	8.02	0.0488
Sn, nM	bdl	bdl	23.2	147	bdl
Ga, nM	bdl	bdl	0.366	2.32	bdl

Table 3: Molar element/Cl ratios for end-member fluids from Buddha's Hands, A1, and bottom seawater.

Vent	Br/Cl×10^{-3}	Na/Cl	K/Cl	Li/Cl×10^{-3}	Rb/Cl×10^{-3}	Cs/Cl ×10^{-6}	Ca/Cl	Sr/Cl×10^{-3}	B/Cl×10^{-4}
Buddha's Hands	1.58	0.802	0.0374	0.870	0.0221	0.115	0.0765	0.219	4.43
A1	1.17	0.809	0.0360	0.809	0.0207	0.219	0.0799	0.111	3.25
Bottom Seawater	1.54	0.861	0.0185	0.048	0.00234	0.00415	0.0188	0.159	7.45

Table 4: REE concentrations (Conc.), corresponding end-member (EM) concentrations in picomol/l (pM), and chondrite-normalized (/Chon.) REE for vent fluids collected at the chimney orifices of Buddha's Hands and A1, respectively.

	Buddha's Hands			A1			Seawater	
	Conc. (pM)	EM (pM)	/Chon.	Conc. (pM)	EM (pM)	/Chon.	Conc. (pM)	/Chon.
La	5117	10724	6.09E-03	394	2505	1.42E-03	29	1.7E-05
Ce	4707	9865	2.17E-03	377	2398	5.26E-04	5.5	1.26E-06
Pr	478	1002	1.47E-03	45.5	289	4.23E-04	4.4	6.53E-06
Nd	1746	3659	1.13E-03	186	1184	3.65E-04	21.4	6.69E-06
Sm	537	1124	1.07E-03	47.6	303	2.89E-04	4.1	3.94E-06
Eu	21936	45979	1.20E-01	1221	7765	2.02E-02	1.1	2.86E-06
Gd	470	985	7.57E-04	37.1	236	1.82E-04	6.3	4.81E-06
Tb	107	223	9.47E-04				0.92	3.91E-06
Dy	272	569	3.65E-04				6.4	4.11E-06
Ho							1.7	4.96E-06
Er	89.5	187	1.88E-04				5.5	5.52E-06
Tm	12.3	26	1.73E-04					
Yb	94.1	197	1.99E-04				5.4	5.46E-06
Lu	6.78	14.3	9.84E-05				0.88	6.06E-06
LREE/HREE			32.8					
Eu/Eu*			133			88		

Note: Reported REE end members were normalized to chondrite (/Chon.). Chondrite data are from Evensen et al. (1978), seawater data are from Douville et al. (1999).

Table 5: Metal content of precipitates collected from the samplers at Buddha's Hands and A1, respectively.

Vent	Fe ppm	Mn ppm	Cu ppm	Co ppm	Ba ppm	Ni ppm	As ppm	Se ppm	Al ppm	V ppm	Zn ppm	Pb ppm	Cd ppm	Ga ppm	Sn ppm
Buddha's Hands	609662	49	60286	3861	1	4.35	55.8	2.35	410	199	97630	402	187	6.52	257
A1	288074	56	17445	439	3	bdl	7.68	bdl	42	9.29	751785	1005	1155	26.9	498

Table 6: Endmember composition of vent fluids from Buddha’s Hands and A1, compared those from other vent fields in different geological setting: Logatchev I (Schmidt et al., 2011), Kairei and Edmond (Gallant and Von Domm, 2006), Von Damm (McDermott, 2015), Rainbow (Charlou et al., 2002; Douville et al., 2002), Nibelungen (Schmidt et al., 2011), TAG (Charlou et al., 1996; Douville et al., 2002), Longqi (Tao et al., 2020), South Cleft (Von Damm and Bischoff, 1987; Palmer and Edmond, 1989; Campbell and Edmond, 1989), North Cleft (Butterfield and Massoth, 1994), Buddha’s Hands, A1 and Seawater: this study.

	Ultramafic-hosted			NTO, Ultramafic-hosted		DF, Mafic-hosted		Mafic-hosted			This study		
	Logatchev I 2007	Kairei 2001	Von Damm 2012	Rainbow 1996	Nibelungen 2006	TAG 1993	Longqi 2020	South Cleft 1984	North Cleft 1990	Edmond 2001	**Buddha’s Hands**	**A1**	Seawater
water depth (m)	3000	2422	2372	2284	3000	3600	2765	2250	2275	3281	**3453**	**3452**	2756
T (°C)	349	315	226	365	>192	363	362	224	324	382	**273**	**272**	2
pH (25 °C)	3.5	3.35	5.56	2.8		3.1	3.32	3.2	2.8	3.13	**5.25**	**6.74**	7.69
CH_4, mM	1.5	0.203	2.81	2.5	1.4	0.147	0.38			0.289	**0.884**		0.0003
H_2, mM	5.8	8.19	18.2	16	11.4	0.37	0.31			0.142	**7.07**		0.0004

H_2S, mM	0.5-0.8	4.07	3.24	1.0	0.035	3-4	5.9	3.5	3.7	4.81			0
Cl, mM	542	571	651	750	551	650	605	1090	908	927	**928**	**303**	542
Br, μM	835	920	1000	1178	840	1045		1832		1390	**1470**	**354**	833
B, μM	333				179		376	491	482		**411**	**98.4**	404
Si, mM	8.6	17.1	7.56	6.9	12.7	20	16	23.3	21	20.8	**1.17**	**1.39**	0.0850
Al, μM		4.35	3.1	2		10		1.9		12.5	**0.869**		
Na, mM	450	492	603	553	473	550	463	796	695	721	**744**	**245**	467
K, mM	23.5	13.3	16.5	20	19.4	18	14	51.6	41	44.2	**34.7**	**10.9**	10
Ca, mM	30.5	28.6	15.7	67	29.6	28	42	96.4	79	63.4	**71**	**24.2**	10.2
Li, μM	227	553	219	340	364	430	680	1720	1570	1050	**807**	**245**	26.2
Rb, μM	27		5.6	37	17.5	9.5	9	37	27.6		**20.5**	**6.28**	1.27
Cs, nM	354			333	231	110	99	368	217		**105**	**66.1**	2.25
Sr, μM	129	70.3	99	200	75.8	103	93	312	236	184	**203**	**33.7**	89.5
Fe, μM	2460	3540	20	24000	4870	5170	11300	18700	4820	13900	**11916**	**365**	0.0291
Mn, μM	356	811	10	2250	877	710	1600	3590	1940	1439	**1550**	**564**	
Cu, μM	43	276	2.9	140	202	130	42			161	**3.39**	**1.59**	

Zn, µM	37.8	66.5	1.6	160	101	83	900	134	**28.2**	**199**	0.0188
Ba, µM				＞67		＞19			**5.53**	**7.79**	0.0897
Cd, nM	40	69.9		130	109	66		261	**39.7**	**224**	
Co, µM	0.94			13	1.52	＜2			**1.23**	**0.590**	
Pb, nM	140	314		48	329	110		1040	**70.8**	**34.5**	
Ag, nM				47		51			**12.7**	**52.4**	
Sb, nM				3.1		3.9			**1.20**	**18.6**	1.91
Tl, nM	15.5			9	12				**4.52**	**8.02**	0.0488
Sn, nM	36				200					**147**	

Note: DF: detachment faults, **NTO: non-transform offset**

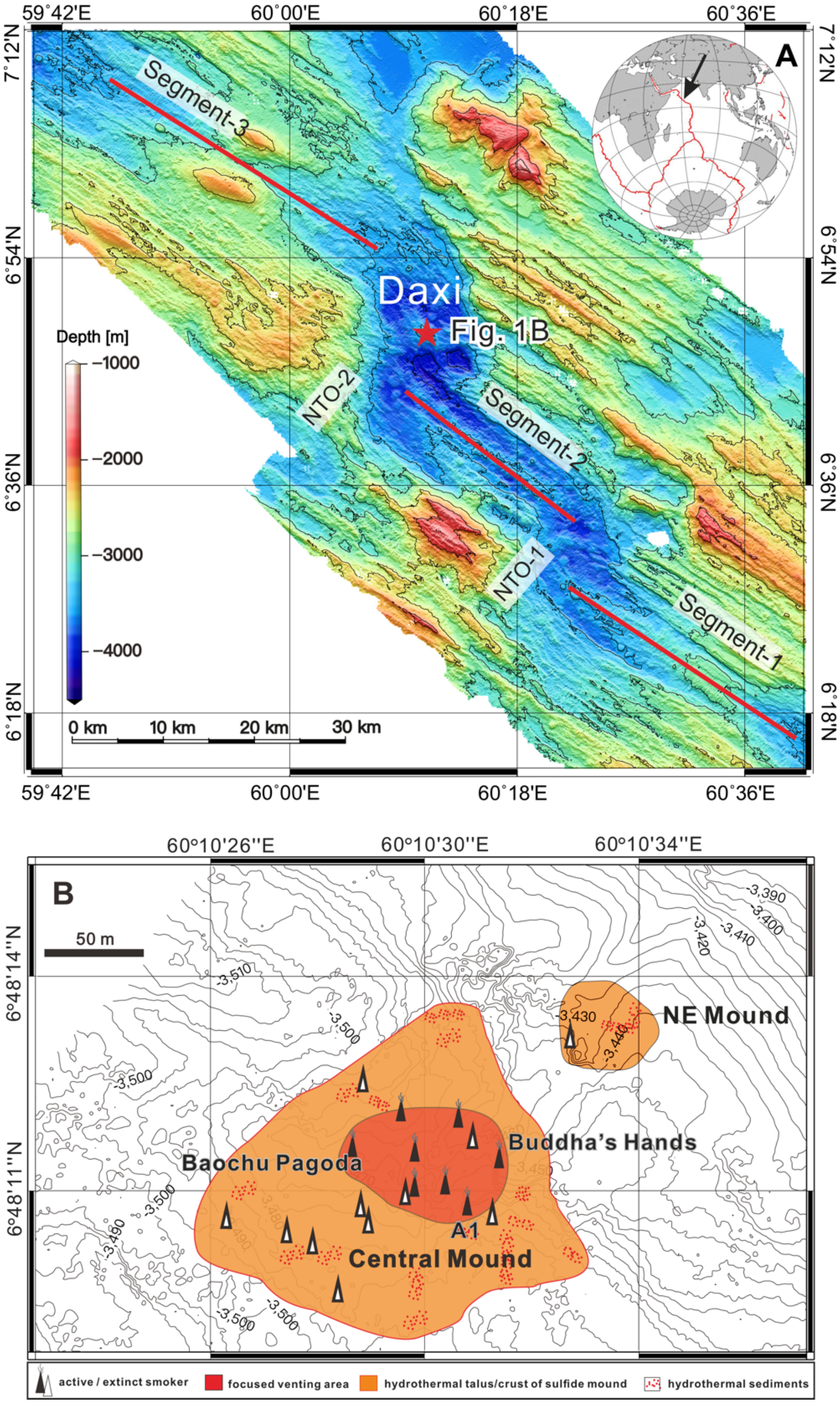

Figure 1 (A): Bathymetry of the study area on Carlsberg Ridge, Northwest Indian Ridge. Red star = Daxi Vent Field. **(B)** Map showing the distribution of active black smokers and extinct chimneys in the Daxi Vent Field; note Buddha's Hands and A1 chimney (modified from Wang et al. 2021).

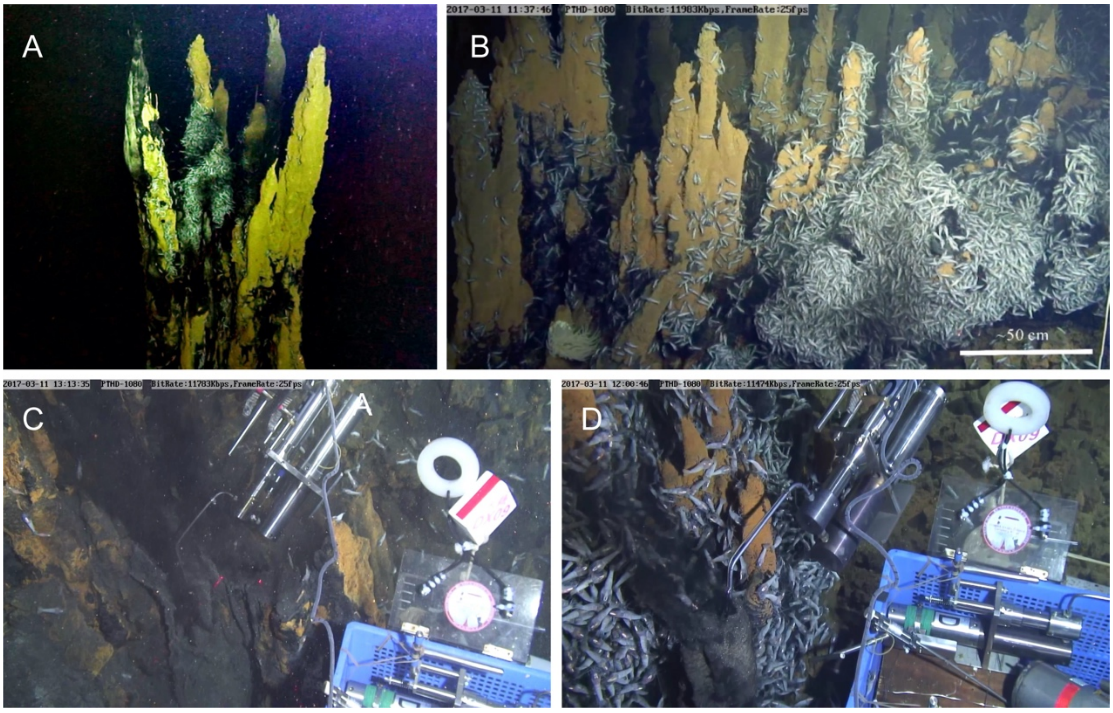

Figure 2 (A): The 20-m high Buddha's Hands sulfide chimney and its pipe-like structures, diffuse venting and dense shrimp assemblage. **(B)** The A1 chimney clusters, several meters high with diffuse fluids and aggregation of hundreds of *alvinocaridid* shrimp **(C)** Sampling the vent fluid at Buddha's Hands using a titanium gas-tight isobaric (IGT) sampler. **(D)** Sampling at A1 using same IGT sampler

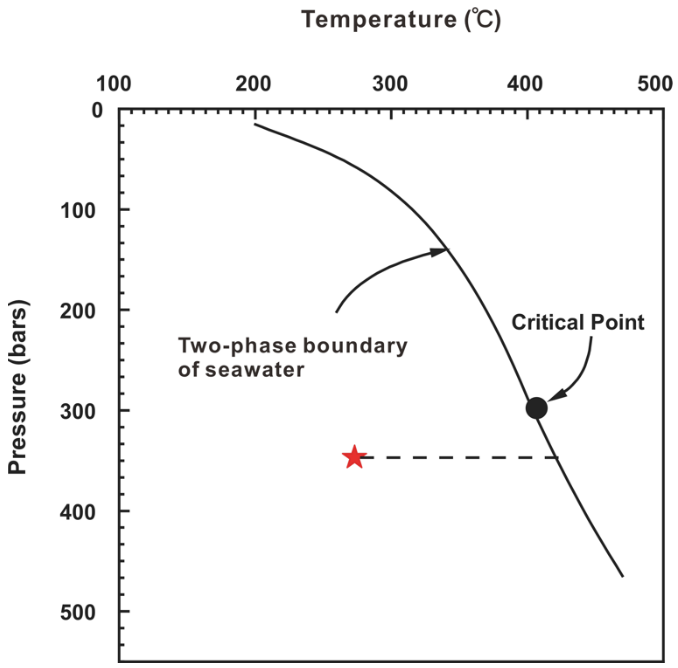

Figure 3: Temperature-pressure phase diagram for the system NaCl-H_2O with the liquid-vapor two-phase boundary of seawater (3.2 wt% NaCl) (Bischoff and Rosenbauer, 1985). The red star indicates P-T conditions of DVF fluids at the seafloor. The black circle indicates the critical point of seawater at 3.2 % NaCl.

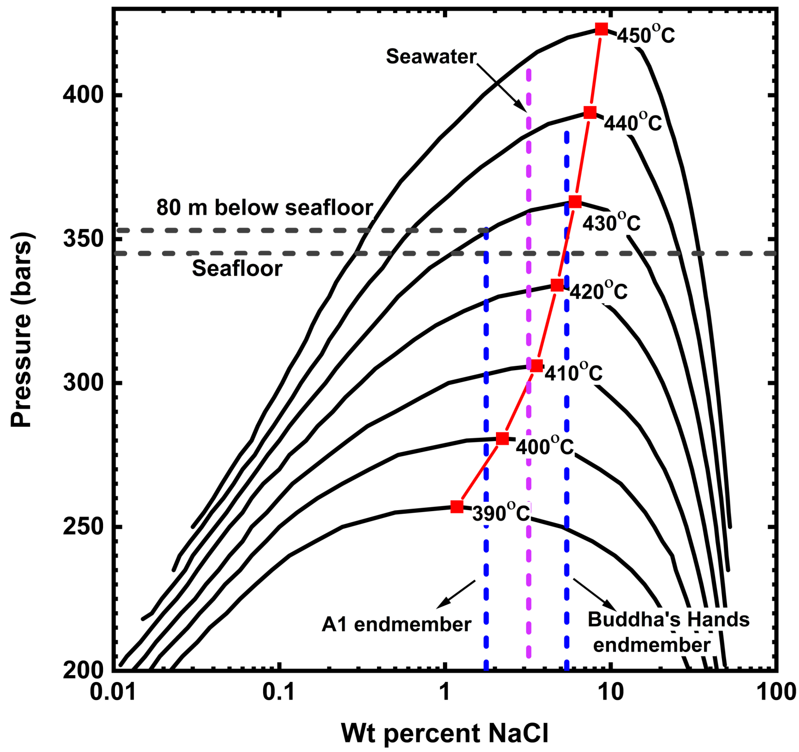

Figure 4: Isotherms of the vapor-liquid region of NaCl-H_2O from 300°C to 500°C (Bischoff and Pitzer, 1989). The red line with squares is the critical line. The endmember wt % NaCl of Buddha's Hands and A1 are shown by the dotted blue vertical line and seawater salinity is shown by the dotted magenta vertical line. The pressure at the seafloor, 80 m and 300 m subseafloor are shown by the black dotted horizontal lines.

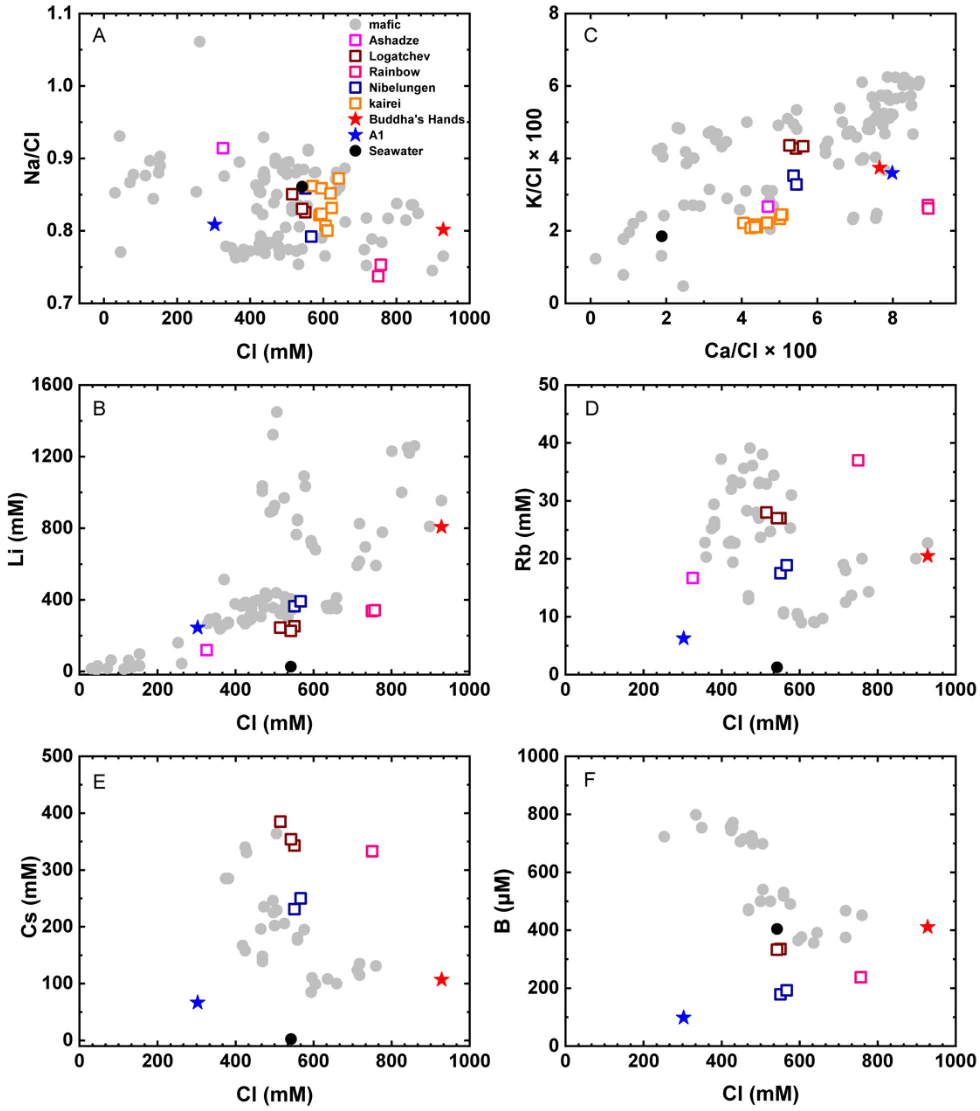

Figure 5: Endmember composition of DVF fluids, compared to vent fluids from other hydrothermal sites. (A) dissolved Na/Cl versus Cl; (B) dissolved K/Cl versus Ca/Cl; (C) dissolved Li versus Cl; (D) dissolved Rb versus Cl; (E) dissolved Cs versus Cl; (F) dissolved B versus Cl. Data sources for mafic-hosted systems (MAR: Lucky Strike, Broken Spur, TAG (BS), TAG (WS), Snake Pit, Menez Gwen; EPR: 9-10°N, 13°N, 21°N, Juan de Fuca Ridge) are from the IEDA EarthChem VentDB chemistry data collection (Mottl, 2012); Longqi (Tao et al., 2020). Data sources for ultramafic-hosted systems: Rainbow (Douville et al., 2002; Charlou et al., 2002); Logatchev (Schmidt et

al., 2007); Nibelungen (Schmidt et al., 2011); Kairei (Gamo et al., 2001; Gallant and Von Damm, 2006; Kumagai et al., 2008); Ashadze (Charlou et al., 2010). Daxi: this study.

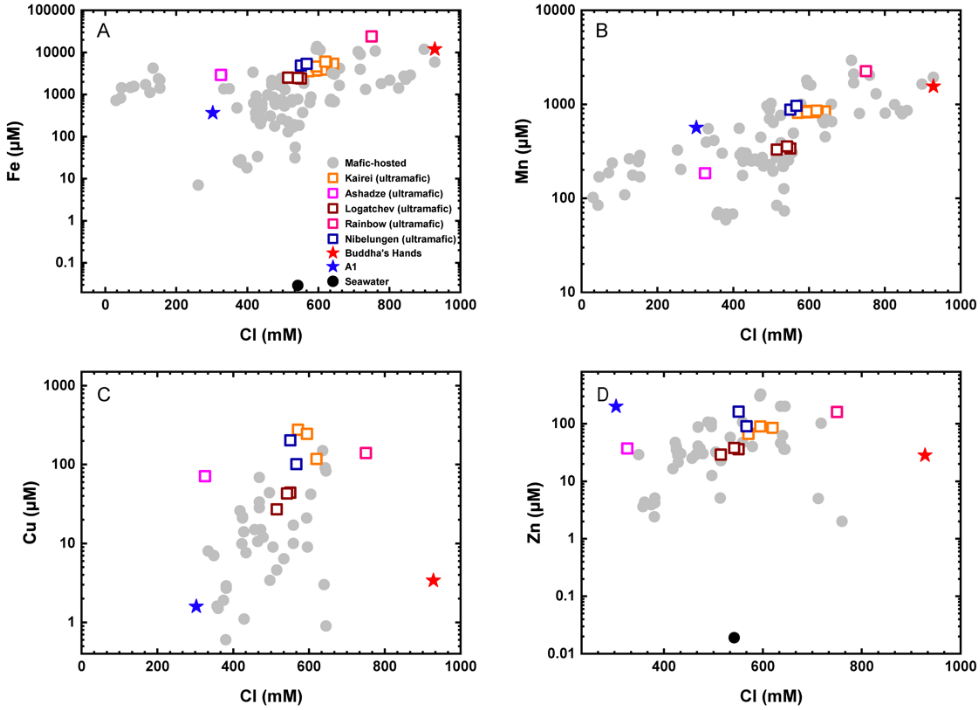

Figure 6: Plot of end-member metal compositions from various hydrothermal fields. (A) dissolved Fe versus Cl; (B) dissolved Mn versus Cl; (C) dissolved Cu versus Cl; (D) dissolved Zn versus Cl. data sources as in Fig. 5.

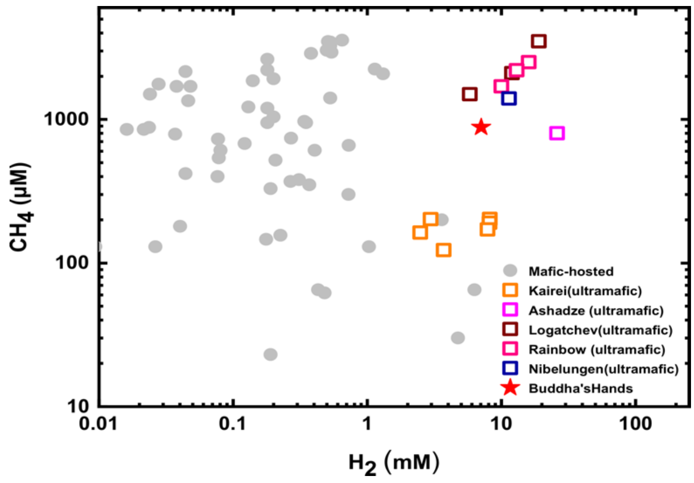

Figure 7: Endmember concentration of dissolved H_2 and CH_4 in hydrothermal fluids; data sources as in Fig. 5.

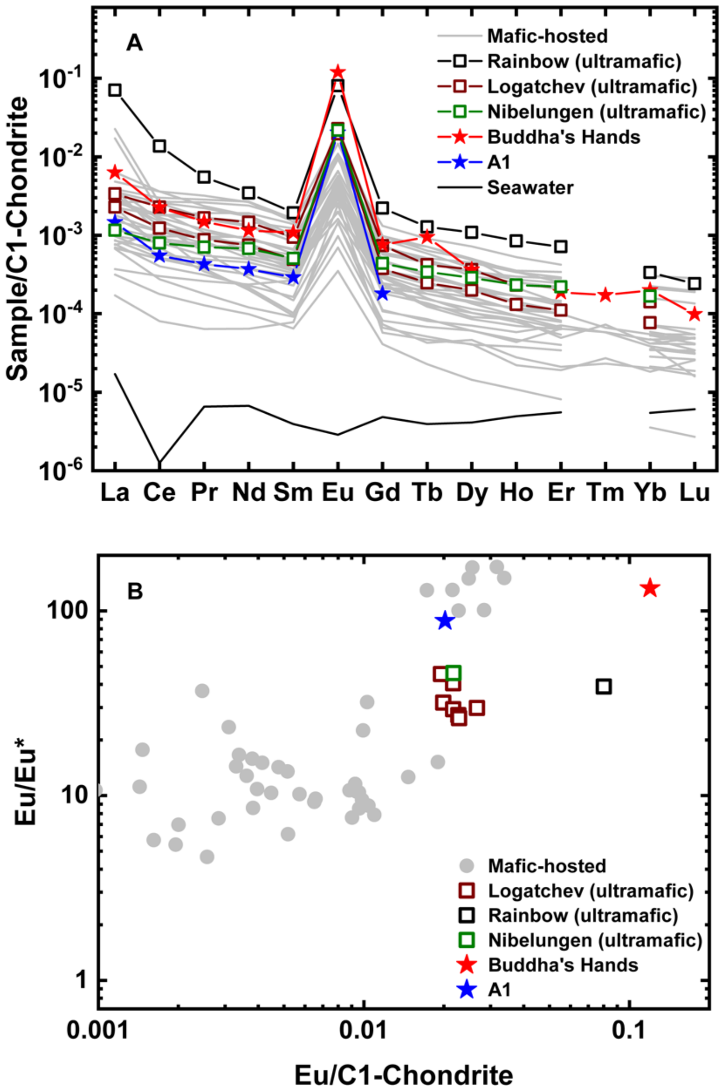

Figure 8: (A) Chondrite-normalized rare earth elements in the Daxi fluids. (B) The Eu anomaly (expressed as Eu/Eu* of chondrite-normalized concentrations) vs Eu/Cl-Chondrite. Data sources as in Fig. 5 and Table 4.

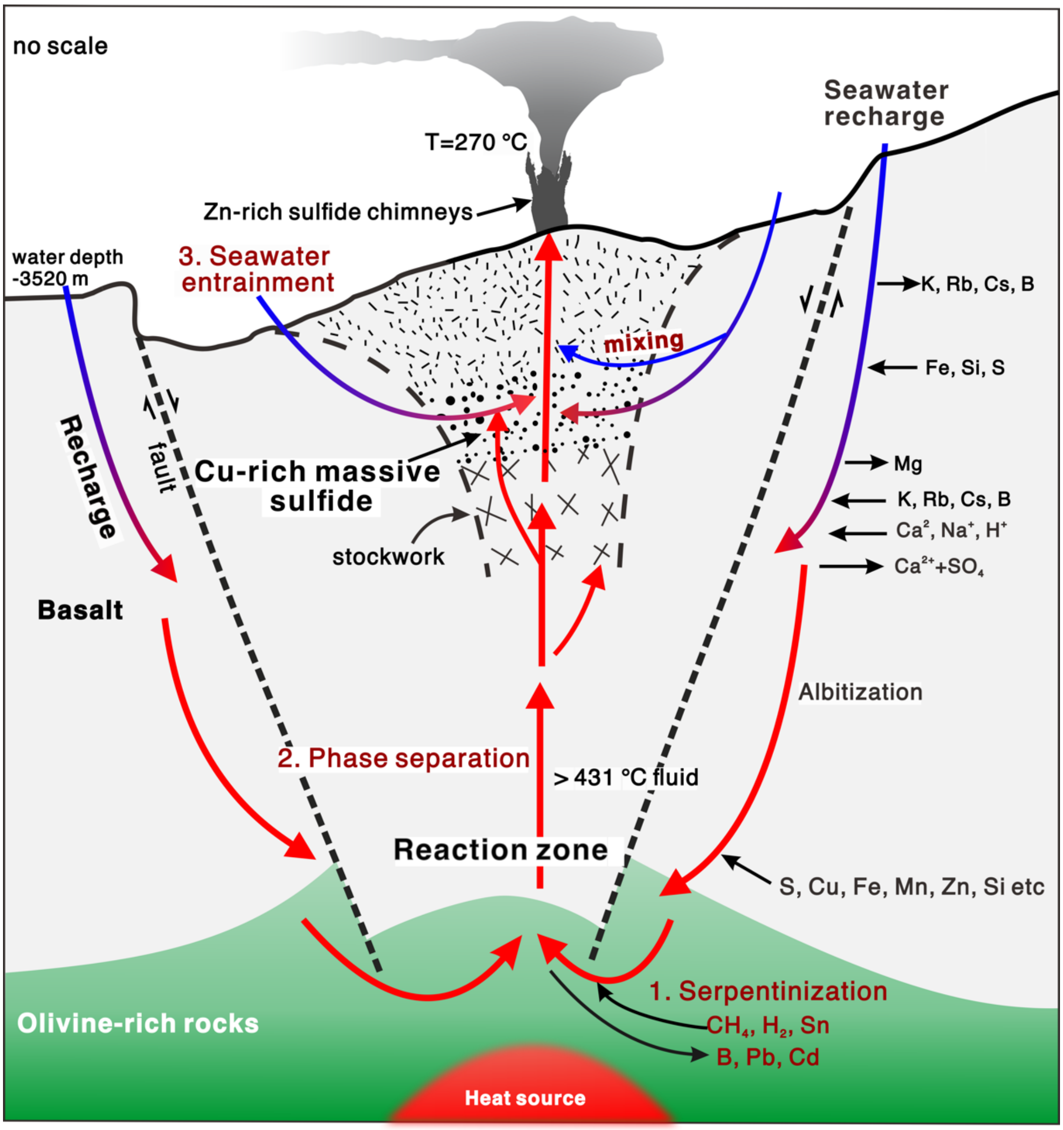

Figure 9: Proposed hybrid hydrothermal system at the DVF interpreting formation and evolution of hydrothermal fluids. (1) As cold seawater penetrates into the crust via recharge zone and reaches the reaction zone, serpentinization is involved, resulting in unusually high H_2 and CH_4 concentrations in the hydrothermal fluid. (2) As the fluid reaches the two-phase curve, phase separation occurs and the fluid separates into a vapor phase and a brine phase. (3) During the following ascent, the resulting 431 °C fluid mixes with entrained cold seawater and is cooled to ~270 °C. Cu-sulfides and Fe-sulfides deposit and generate secondary acidity during mixing. The Zn concentration in the fluid is elevated due to remobilization and result in the deposition of Zn-sulfides.